

**INVESTIGATION OF LEACHING CHARACTERISTICS
OF COAL ASH**

**A
THESIS**

Submitted in partial fulfillment of the requirements for the award of degree of

Master of Engineering (M.E.)

**In
Thermal Engineering**

**Submitted by
NAKUL SHARMA
(ROLL NO. 801283017)**



Under the guidance of

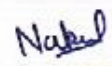
**Dr. S.K. MOHAPATRA
(Senior Professor, DOAA)**

**DEPARTMENT OF MECHANICAL ENGINEERING
THAPAR UNIVERSITY, PATIALA – 147004**

JULY 2014

DECLARATION

I hereby declare that thesis entitled " Investigation of leaching characteristics of Coal ash" is an authentic record of my study carried out as requirements for award of the degree of M.E (Thermal Engineering) at Thapar University, Patiala, under the supervision of Dr. S.K. Mohapatra, DOAA & Senior Professor, Department of Mechanical Engineering, Thapar University, Patiala. The matter presented in this thesis has not been submitted for the award of any other degree of this or any other university.


(NAKUL SHARMA)

This is to certify that the above declaration made by the student concerned is correct to best of my knowledge and belief.


(Dr. S.K. MOHAPATRA)

DOAA & Senior Professor,
Thapar University, Patiala

Countersigned by


(Dr. AJAY BATISH)

Professor & Head

Department of Mechanical Engineering

Thapar University, Patiala-147004


(Dr. S.K. MOHAPATRA)

Dean of Academic Affairs

Thapar University, Patiala-147004

ACKNOWLEDGEMENT

At first, thanks to the almighty for his abundant blessing showered on me throughout this endeavour to complete this work successfully.

My honorable guide Dr. S.K Mohapatra, Senior Professor, Department of Mechanical Engineering, is a person to whom I shall always remain grateful for his excellent guidance, valuable discussions, encouragement, constructive criticism and his insights have strengthened this study significantly. He gave me a complete freedom to use my opinion, correcting whenever necessary in my dissertation.

I would like to thanks to Dr. Ajay Batish, Head of the Mechanical Engineering Department, and Mr. Satish Kumar, Assistant Professor, Mechanical Engineering Department, Thapar University Patiala, who has been supportive at all times and accommodative.

I acknowledge my sincere thanks to all my friends and classmates for providing the companionship and making my stay at Thapar University, Patiala pleasant and joyful.

Last but not the least; I would like to express my love and affection towards my parents and younger brother for their constant moral support and encouragement throughout my life.



Nakul Sharma

ABSTRACT

The present study on the investigation of the mineralogical and physio-chemical properties of fly ash was conducted at the MED Department, Thapar University, and Patiala. Three Fly ash samples were taken from three different thermal power plants namely Ropar, Hisar and Bhatinda Thermal Power stations of varied specific gravity and densities. Leaching Tests on Coal ash was performed using TCLP (Toxicity leaching procedure) approach at Mechanical Engineering Department and for studying Physical properties of Coal ash Tests such as XRD (X-ray diffraction), DTA (Differential Thermal analysis), SEM (Scanning Electron Microscopy) and EDS (Energy Dispersive Spectroscopy) were performed on three samples of Fly and Bottom ash. It was observed from XRD tests that these samples consist mainly of minerals such as Quartz, Mullite, Hematite and kyanite as their main constituents along with traces of other components. Volume fraction was calculated to determine the content of these minerals in Coal ash. XRD peaks showed that these Minerals were mostly in crystalline phase. EDS tests were performed on samples with and without Leachates. Samples without Leachate showed Silicon (Si), Aluminum (Al) and Iron (Fe) as main constituents along with traces of Titanium (Ti), Potassium, Calcium (Ca) and Zirconium (Zr) and Samples with Leachates showed reduction in content of these elements due to leaching. Also SEM (Scanning Electron Microscopy) tests were performed on Coal ash leachates and Coal ash without leachates. It revealed the changes in morphology from uniform, spherical glassy spherical particles (in case of non-leachates) to less uniform, irregular and coarse particles with changes in shape and size (in case of leachates). Lastly AAS (Atomic absorption spectroscopy) was performed on Bhatinda fly ash leachate. Results revealed concentration (mg/l) of some elements such as Cd (Cadmium), Cr (Chromium), and Pb (Lead) well above the WHO limit on drinking water.

CONTENTS

Chapters	Title	PageNo.
	LIST OF FIGURES	iii
	LIST OT TABLES	v
	LIST OF SYMBOLS	vi
	LIST OF ABBREVIATIONS	vii
	NOMENCLATURE	viii
Chapter-1	INTRODUCTION	
1.1	Types of coal ash	1
1.2	Fly ash utilization	2
1.3	Features	2
1.4	Classification of fly ash	3
1.5	Generation of coal ash	3
1.6	Leaching	6
1.6.1	Factors affecting Leaching	6
Chapter-2	LITERATUREREVIEW	
2.1	Leaching and Physical Characteristics of Coal ash	8
Chapter-3	CHARACTERIZATION STUDIES OF COAL ASH	
3.1	Particle size distribution	20
3.2	Scanning Electron Microscopy(SEM) analysis	22
3.3	Energy Dispersive Spectroscopy (EDX) analysis	26
3.4	Mineralogical Properties of Coal Ash	31
3.5	Thermal Analysis of Coal Ash	38

4.1	Description of equipment	46
4.2	Experimental procedure	46
4.3	Atomic absorption spectroscopy	47
4.4	SEM analysis of fly ash leachates	48
4.5	EDS analysis of fly ash leachate samples	50
4.6	EDS analysis of bottom ash leachate samples	53
4.7	SEM images of bottom ash leachates	55
Chapter-5	CONCLUSIONANDFURTHERSCOPE	
5.1	Conclusions	58
5.2	Future Scope	58
	REFERENCES	59

LIST OF FIGURES

Figure no	Description	Page no
Fig 1.1	Typical Example of Coal Ash generation	5
Fig 1.2	Toxicity testing procedure	7
Fig 3.1	Sieve analysis Machine	21
Fig 3.2	PSD Graph for 3 Samples of Fly Ash	21
Fig 3.3	PSD Graph for 3 Samples of Bottom Ash	22
Fig 3.4	SEM image of S-III Fly ash (at 2000X)	23
Fig 3.5	SEM image of S-I Fly ash (at 2000X)	23
Fig 3.6	SEM image of S-II Fly ash (at 2000X)	24
Fig 3.7	SEM image of S-III Bottom ash (at 2000X)	24
Fig 3.8	SEM image of S-I Bottom ash (at 2000X)	25
Fig 3.9	SEM image of S-II Bottom ash (at 2000X)	25
Fig 3.10	EDS spectrum of S-III Fly Ash	27
Fig 3.11	EDS spectrum of S-I Fly Ash	27
Fig 3.12	EDS spectrum of S-II Fly Ash	27
Fig 3.13	EDS spectrum of S-III Bottom Ash	29
Fig 3.14	EDS spectrum of S-I Bottom Ash	29
Fig 3.15	EDS spectrum of S-II Bottom Ash	29
Fig 3.16	XRD peaks of S-II Fly ash	32
Fig 3.17	XRD peaks of S-III Fly ash	33
Fig 3.18	XRD peaks of S-I Fly ash	34
Fig 3.19	XRD peaks of S-II Bottom ash	35
Fig 3.20	XRD peaks of S-III Bottom ash	36
Fig 3.21	XRD peaks of S-I Bottom ash	37
Fig 3.22	DTA/TG graph of S-III fly ash	39
Fig 3.23	DTA/TG graph of S-I fly ash	40
Fig 3.24	DTA/TG graph of S-II fly ash	40
Fig 3.25	DTA/TG graph of S-III bottom ash	43
Fig 3.26	DTA/TG graph of S-I bottom ash	44

Fig 3.27	DTA/TG graph of S-II bottom ash	44
Fig 4.1	SEM-JSM-6510LV JEOL MODEL	46
Fig 4.2	AAS (GBC)	47
Fig 4.3	SEM ANALYSIS OF S-III FLY ASH LEACHATE	48
Fig 4.4	SEM ANALYSIS OF S-I FLY ASH LEACHATE	48
Fig 4.5	SEM ANALYSIS OF S-II FLY ASH LEACHATE	49
Fig 4.6	EDS ANALYSIS OF S-III FLY ASH LEACHATE	50
Fig 4.7	EDS ANALYSIS OF S-I FLY ASH LEACHATE	50
Fig 4.8	EDS ANALYSIS OF S-II FLY ASH LEACHATE	51
Fig 4.9	EDS SPECTRUM OF S-III BOTTOM ASH LEACHATE	53
Fig 4.10	EDS SPECTRUM OF S-I BOTTOM LEACHATE	53
Fig 4.11	EDS SPECTRUM OF S-II BOTTOM LEACHATE	54
Fig 4.12	SEM IMAGE OF S-III BOTTOM ASH LEACHATE	55
Fig 4.13	SEM IMAGE OF S-I BOTTOM ASH LEACHATE	55
Fig 4.14	SEM IMAGE OF S-II BOTTOM ASH LEACHATE	56
Fig 4.15	AAS RESULTS OF S-III FLY ASH LEACHATE	57

LIST OF TABLES

Table no	Description	Page no
1.1	Coal Consumption and Ash generation	4
1.2	Fly ash generation, utilization in different countries	4
3.1	Composition of Fly ash Samples	28
3.2	Composition of Bottom ash Samples	30
3.3	Mineralogical Composition of S-II Fly ash	32
3.4	Mineralogical Composition of S-III Fly ash	33
3.5	Mineralogical Composition of S-I Fly ash	34
3.6	Mineralogical Composition of S-II Bottom Ash	35
3.7	Minerological Composition of S-III Bottom ash	36
3.8	Minerological Composition of S-I Bottom Ash	37
4.1	Chemical composition of fly ash leachates	52
4.2	Chemical composition of bottom ash leachates	54
4.3	IS:10500 limit on Drinking water	57

LIST OF SYMBOLS

Fe	: Iron
Si	: Silicon
Cu	: Copper
Pt	: Platinum
Cd	: Cadmium
Al	: Aluminum
Cr	: Chromium
Hg	: Mercury
Ni	: Nickel
Mo	: Molybdenum
Pb	: Lead
Ca	: Calcium
O	: Oxygen
Ba	: Barium
Zn	: Zinc
Mn	: Manganese
Mg	: Magnesium
Q	: Quartz
H	: Hematite
M	: Mullite
C	: Corundum
K	: Kinamite

ABBREVIATIONS

ASTM	: American society for testing materials.
XRD	: X-ray diffraction.
SEM	: Scanning electron microscopy.
PSD	: Particle size distribution.
AAS	: Atomic absorption spectroscopy.
DTA	: Differential thermal analysis.
TGA	: Thermo-gravity metric analysis.
TCLP	: Toxicity characteristic leaching procedure.
SA	: South African.
CO	: Columbian.
XRF	: X-ray fluorescence.
LOI	: Loss on ignition.
PM	: Particulate matter.
EDS	: Energy dispersive spectroscopy.
EPA	: Environmental protection agency.
INAA	: Instrumental neutron activation analysis.
ICP-MS	: Inductive coupled plasma mass spectroscopy.
PM	: Particulate matter.
O/C	: Oxygen by Carbon.

BET	: Brunauer–Emmett–Teller.
ESP	: Electro static precipitator.
CFBC	: Circulating fluidized bed combustion.

NOMENCLATURE

α	: Alpha
μm	:Micro-meter
2θ	:Bragg angle
Wt.%	:Weight percentage
s	: Sampler
r	:Reference
S-I	:Hisar ash sample
S-II	:Bhatinda ash sample
S-III	: Ropar ash sample

Thermal power plants generate fly and bottom ash from the burning of pulverized coal in large quantities. There are about 125 thermal power plants in India, which form the major source of fly ash in the country. The current trend is that around 150 million tons of fly ash are produced annually in India (2012) and is expected to reach 200 million tons by the year 2020. This has posed a serious threat to our environment and large tracts of available land area. Although fly ash has found its applications in many domains such as Concrete, Building industry, Soil stabilization etc., only a small percentage of the total fly ash produced is being utilized in our country. One of the aims in the present study is the investigation of Physio-Chemical and mineralogical properties of the fly and bottom ash because it provides reliable information about its adverse environmental impacts and its significance as a supplemental material for Future use in various types of industries.

1.1 TYPES OF COAL ASH

- **Fly Ash:** It remains one of the important by-products generated by the combustion of coal in thermal power plants. It is collected from the Electro-static precipitators in dry form. It consists of finest Coal Ash particles and generally consists of oxide material of aluminum-silicate and ferrous type along with it also contains Ca, Mg, K, Ti, C and many other elements in trace proportions.

- **Bottom Ash:** Bottom ash is an incombustible residue procured from the bottom of Boiler furnaces. Bottom ash is coarser than fly ash and mostly composed of fine gravel. The type of by-product produced depends on the type of furnace used to burn the coal.

- **Pond Ash :** Bottom ashes and Fly ash are mixed together with water to form slurry which is pumped to the ash pond area. In the ash pond the ash gets settled and excess water is poured out. This settled ash is called pond ash.

1.2 FLY ASH UTILIZATION: Fly ash finds its application in many industries. Some of them are as follows:

- Fly ash as raw material for cement manufacture.
- Fly ash in Road Embankments
- Fly ash use in pavements
- Fly ash use as pozzolans for replacement of Cement.
- Use in Ceramic Products.
- Pavement Blocks.
- Increases Strength in Concrete.
- Use as Herbicide.

1.3 FEATURES

- **Spherical Shape:** Fly Ash consists mostly of Spherical particles. This property allows it to easily blend it with other mixtures and easy flow, making it as an easy replacement for Cement.
- **Higher Strength:** On combination with free lime, increases structural strength over time.
- **Decreased Permeability:** Increased density and long term pozzolanic action of fly ash, which ties up free lime, results in fewer bleed channels and decreases permeability.
- **Reduced Slump Loss:** More dependable concrete allows for greater working time, especially in hot weather.

- **Reduced Shrinkage:** The largest contributor to drying shrinkage is water content. The lubricating action of fly ash reduces water content and drying shrinkage.

1.4 CLASSIFICATION OF FLY ASH

Two classes of fly ash are defined by ASTM C618: Class F fly ash and Class C fly ash. The main difference between these classes is the amount of elements present such as Silica, Alumina and iron content.

- **Class C Fly Ash:** Fly ash produced from the burning of sub-bituminous coal is known as Class C Fly Ash. It possesses pozzolanic properties and also some self-cementing properties. In the presence of water, Class C fly ash will gain strength over time. It generally contains more than 20% lime (CaO). It does not require an activator. It also contains large amount of alkali contents such as CaO, Fe, Al, Si etc.
- **Class F Fly Ash:** It results from the harder Bituminous Coal. It consists of glassy silica and alumina and in addition to it also requires an activator such as lime in the presence of water to become harder and gain strength over time for the production of cementitious compounds.

1.5 GENERATION OF COAL ASH

Fly ash is produced by Thermal power plants. Generally, coal is pulverized and blown with air into the boiler's chamber where ignition takes place, generating heat in the process and producing a molten byproduct residue. Boiler tubes extract heat from the boiler causing the molten product to harden and form ash particles. Ash particles which are coarser and heavy is referred to as bottom ash, fall to the bottom of the Boiler, whereas the lighter fine ash particles termed as fly ash remain embedded in the flue gas. Prior to exhausting the flue gas, fly ash is removed by particulate control devices known as electrostatic precipitators. Depending upon the source and constituents of the coal being burned, the components of fly ash vary considerably, but to sum up fly ash includes substantial amounts of silicon dioxide (SiO₂), alumina and calcium oxide (CaO), both being indigenous elements

in many coal containing rock layers. In India ash content in the coal is in the range of 30-40%.

Table 1.1 Thermal Power Generation, Coal Consumption and Ash generation in India

Year	Power Generation (mW)	Coal Consumption(Million Tonnes)	Ash Generation (Million Tonnes)
2000	75000	250	95
2010	100000	300	115
2020	138000	400	145

Table 1.2 Fly ash generation and utilization in different countries (2005/06)

S.no	Country	Ash Production, MT	Ash Utilization
1.	India	120	38%
2.	China	110	45%
3.	USA	85	65%
4.	Germany	50	85%
5.	France	6	85%

Major portion of fly ash is used in the cement industry only, whereas some small quantities are used for making fly ash bricks, Agriculture, Landfills. As per the table, Utilization of fly ash has been on increase year by year. Further Desire about controlling pollution to cement Industry can make sure that Fly ash can be put to 100% utilization in the most environmental and economic friendly manner.

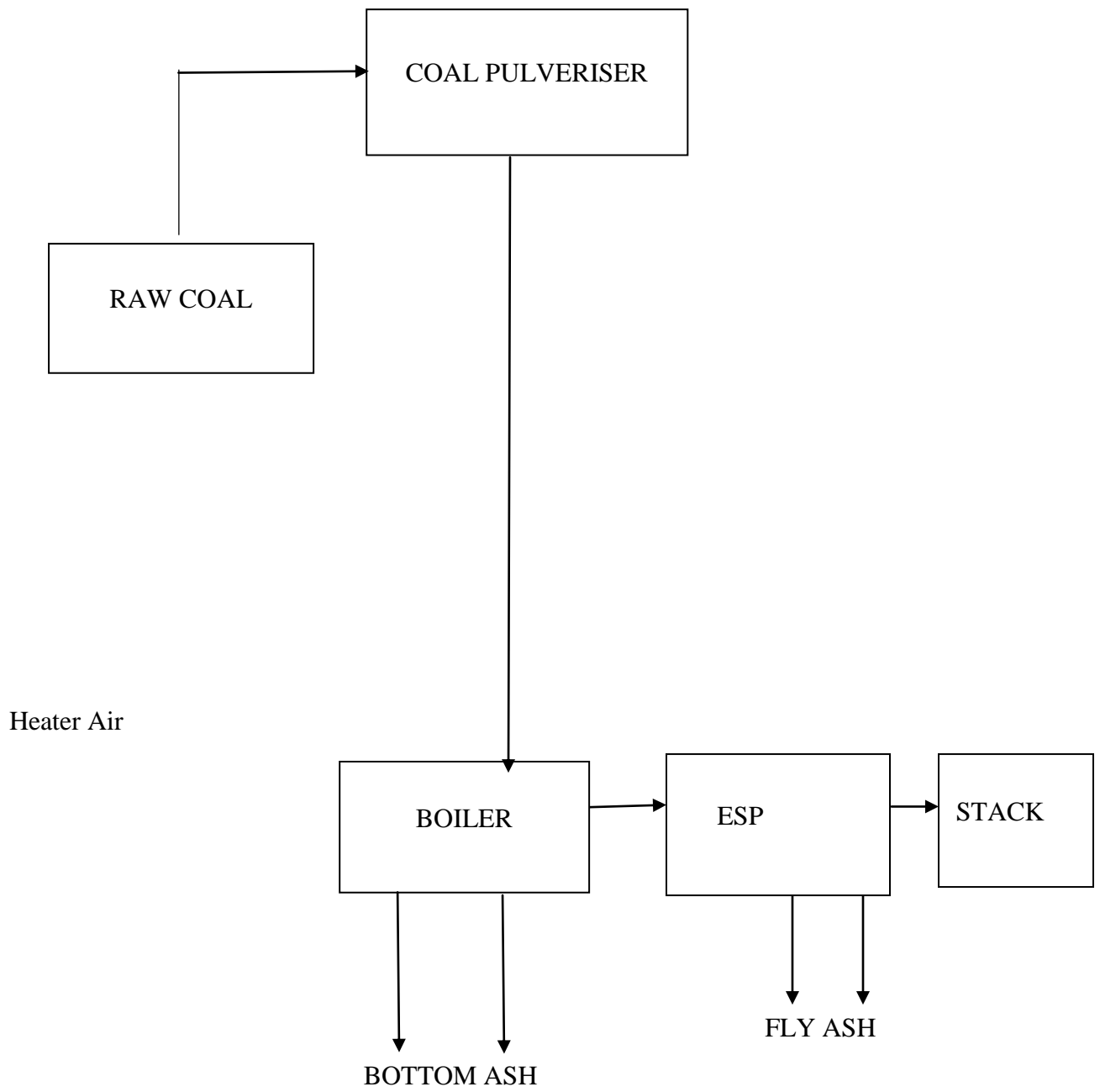


Fig. 1.1 Typical example of coal ash generation

1.6 LEACHING

Leaching is the process of extracting minerals from a solid by dissolving them in a liquid, either in natural form or through an artificial process. In Leaching components of a solid material are released into a contacting water phase. Although some species may be more of an ecological concern than others, leaching process is indiscriminant such that all constituents (inorganic, organic contaminants) are released under a common set of chemical processes which include mineral dissolution, desorption and complexation and mass transport processes. These phenomena are affected by certain factors that can alter the rate or extent of leaching.

Describing leaching by a very simple equation:

Material (leachee) + leachant → leachate

1.6.1 FACTORS AFFECTING LEACHING

- Internal chemical and physical reactions.
- External factors from the surrounding environment.
- Physical degradation of the solid constituent due to erosion or cracking.
- Loss of constituents due to the leaching process itself.

1.6.2 TOXICITY TESTING PROCEDURES

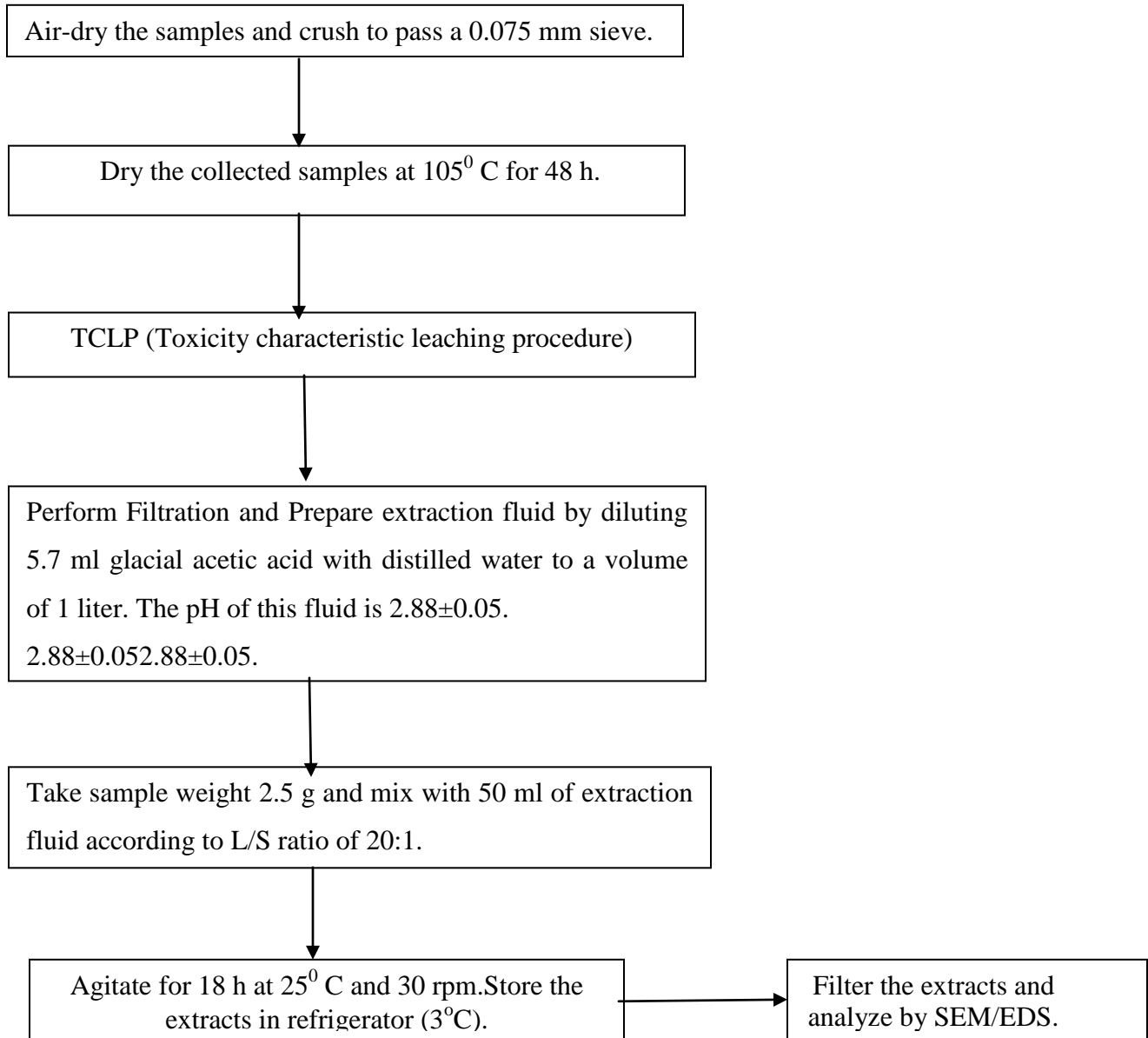


Fig 1.2 Toxicity testing procedure

A lot of work has been done in the past to investigate Physio-Chemical and Mineralogical properties of the fly ash. Various Tests such as XRD (X-ray Diffraction), SEM (Scanning Electron Microscopy) have been performed by the researchers. In the present study a wide review of the published works in the field of Mineralogy and Chemical analysis of Coal ash with an emphasis on the analysis of different elements that make up the Fly ash were undertaken and the view of published works are presented in this chapter.

2.1 MINEROLOGICAL AND CHEMICAL ANALYSIS OF COAL ASH

Sakorafa et al. (1995) studied mineralogy, morphology, geochemistry and physical characteristics of fly ash from the Megalopolis lignite fields, Peloponnese (Greece). The primary mineral species present in the fly ash were identified as quartz, anhydrite, plagioclase, hematite, gehlenite and calcite and those present in trace amounts were lime, alkali feldspars, gypsum, mica and unburnt lignite. They established mineralogical composition of fly ash using SEM-JSM 840 instrument and found that fly ash consists of irregularly shaped spherical particles. They traced elements such as As, Cd, MO and Se, and Ni, V and Zn using AAS (Atomic absorption Spectroscopy) Philips PW 1404 apparatus and the results obtained were compared with those of reference elements. Furthermore they also found that elemental compositions of fly ash samples studied were very similar. Main inorganic elements present in the fly ash were Silicon and Aluminum. CO_2 and SO_3 contents were determined by the Leco CHN 600 and Leco SC 132 instruments according to the ASTM D3176-84 and D4239-85 methods respectively.

Stanislav et al. (1995) studied the phase-mineralogical and chemical composition of solid waste products from coal combustion. Samples of Fly ashes, bottom ashes and lagoon ashes from eleven Bulgarian thermoelectric Power stations were taken and studied thoroughly. It

was observed that inorganic part consists mainly of amorphous components and lesser amounts of crystalline components. They recorded X-ray Diffraction pattern using Diffractometer with Co and Cu $K\alpha$ radiation. They also conducted DTA (Differential Thermal Analysis) TGA (Thermo gravity metric analysis) in an atmosphere up to 1500°C. Samples were prepared from powder pellets for SEM examination. They also categorized mineral composition, morphological and microstructural characteristics of particle material as well as some genetic phase peculiarities. They demonstrated that when there is detailed information on the modes of mineral occurrence in coal and their behavior during heating, it is possible to make a reliable prediction of the formation of the waste products during coal burning and gasification.

Bayat (1997) studied mineralogical, morphological, physical and chemical properties of seven different fly ashes collected from eastern, central and western lignite and bituminous coal fields in Turkey. He also analyzed mineral matter in the fly ashes using X-ray diffraction and found contents such as anhydrite, lime, quartz and hematite + ferrite spinel. He found that much higher calcium concentrations in these samples result in the formation of lime (CaO), melilite $[(Ca,Na)_2(Mg,Al,Fe)(Si,Al)_2O_7]$ and merwinite $[Ca_3Mg(SiO)_4]$. He also detected the presence of anhydrite in all samples which indicated the high activity of calcium not only promotes the formation of sulfates from calcite in the presence of sulfur and oxygen, but also the dehydration of gypsum during and after combustion, occurring at temperatures above 400-500°C. He made it clear from the microscopy data that some of the dominant particles irregularly formed, vesicular particles with some well-formed individual spheres in Catalagzi and Tuncbilek fly ashes. About 55-80 wt. % with less than 45 pm in size for Yatagan, Soma, Yenikoy and Afsin- Elbistan fly ashes was found. He revealed after performing chemical analyses of the fly ashes that they were mainly composed of CaO, SiO₂ and Al₂O₃. These fly ashes have a potential use in wastewater treatment since they can be easily obtained in large quantities at low price or even without price. Moreover, the fly ashes could be also used as a liming material to raise the low pH of acid soils in humid regions, such as around the Black Sea coast of Turkey.

Swapan et al. (1997) studied phase mineralogy and leaching characteristics of some Indian coal fly ashes for evaluating their safe disposal in abandoned coal mines. They conducted leaching tests of fly ash using strong acid/alkali solutions and distilled water under different conditions (solid liquid ratio, leaching time, pH) in the temperature range of 30-100°C. After test they confirmed the concentration of various metals in leachates depends on their chemical nature, association with mineral phases of ash and follows the similar concentration profile to that of iron, especially in acidic medium. They also found that distribution of toxic trace elements in fly ash and their leach ability depended on the amount of unburnt carbon and iron in fly ash. In alkaline medium, leaching of iron and toxic trace elements (except Arsenic) from fly ash was very negligible. Hence they stated that alkali treatment of coal fly ash is desirable for its safe use in refilling of coal mines.

Nathan et al. (1998) carried out two compliance tests one is the European CEN/TC192 and other the US TCLP 1311 methods. They established the results and showed that the TCLP 1311 method is more appropriate for testing the alkaline fly coal ash produced in Israel. The fine particles and particularly the very fine particles (<1 µm) in coal ash play an important role above their weight concentration because of their large active surface area. This is significant both for leaching and physical properties. They used computerized scanning electron microscope feature analysis to characterize these particles and to determine their distribution among the different small grain sizes in two industrial fly coal ashes. While the results are not quantitative, they add considerable knowledge to coal fly ash characterization.

Henry et al. (1998) describes a comprehensive study of some samples of Israel fly ash, with the purpose of elucidating their chemical, physical, mineralogical and technical properties as an incentive to their utilization. Also two representative samples of coal fly ash from Israel were available. Samples were prepared by The Coal Ash Administration, ash. These fly ashes are supposedly representative of the vast bulk of the fly ash produced. They also obtained the results on these samples ('South African' (SA) and 'Colombian' (CO) and showed that the materials are of good quality (especially SA) and have considerable economic potential.

Kolay et al. (2000) carried out experimental investigations for analyzing physio-chemical and mineralogical properties of cenospheres of an ash lagoon. They collected floating material on the ash lagoon from Dahanu Thermal Power Plant, Maharashtra, India. Then they mixed sample with water and made to pass through centrifuge at 4000 rpm for a duration of 30 min. Afterwards they filtered the material floating on the water surface and oven-dried. They analyzed chemical composition of the sample through X-ray fluorescence (XRF) setup and SEM, XRD and TGA of the sample was taken and particle size distribution (PSD) of the cenospheres were obtained.

Moreno et al. (2004) characterized European pulverized fly ashes obtained from Spain, Netherlands, Italy and Greece in terms of their chemical composition, mineralogy and physical properties. They determined the amount and composition of the glass. It was found that the materials analyzed have varied compositions and were for determining their suitability in different applications. The results were compared to the literature to determine their similarities to UK coal fly ashes. Also they performed Chemical analysis which enabled the categorization of the ashes based on their oxide contents. Based on leaching tests, they came to know that certain ashes were identified as having limitations for some further uses due to the detection of relatively high levels of leachable trace elements. Density was observed and stated that these are related to factors such as mineralogical content and particle morphology.

Grochowia et al. (2004) studied the influence of selected properties of fly ash on the measurements of an on-line analyzer. The samples were taken using an inspection method within a period of 3 months. Systematic observation of the properties of the ash allowed monitoring of the work of the industrial analyzer during a relatively long period of the power plant work. They examined samples of coal fly ash for their chemical and physical properties. Morphology was done by scanning electron microscopy (SEM). Finally they determined unburned carbon content in fly ash using loss-on-ignition (LOI) and thermogravimetry analysis (TGA). Also particle size distribution of fly ash was examined

and they discussed correlation between laboratory and on-line industrial measurements of the unburned carbon content of ash.

Goodarzi (2005) studied the total particulates (PM) and size fractions PM₁₀, PM₁₀, and PM_{2.5}. He carried out sampling following EPA Method 201A and he performed three tests at each station. He also examined emitted particles using SEM/EDX and gravimetric method for finding their sizes. Afterward's elemental composition of particles was determined using INAA and ICP-MS. Classification of particles were done based on their morphologies and chemistries which revealed the following minerals such as unburnt carbon, quartz, and by-products of the dissociation, fractional process and contamination by minerals in coal. It was found that the emitted particles were mostly spherical and their matrices are composed of aluminosilicate minerals containing calcium. The PM₁₀ fraction contains small microspheres, fragments of char, and angular quartz and feldspar particles. The PM₁₀ fraction contains solid spheres and cenospheres, gypsum needles, and particles of char. The PM_{2.5} particle size fraction is mostly composed of solid spherical aluminosilicates with some surface enrichment of elements such as Ba, Ca, and Fe.

Brodowski (2005) studied BC (Black Carbon) in particle-size and density fractions of the surface soil of a Haplic Chernozem using a scanning electron microscope (SEM) coupled to an energy-dispersive X-ray spectrometer (EDX) for investigating the morphological and chemical properties of BC as a function of its origin and fate in soils. He established the results and showed that BC occur as SEM-amorphous particles. It was observed that the BC particles exhibited different morphologies ranging from spherical to irregular shapes and from smooth to rough surfaces. He ascertained the identity of BC by atomic O/C (Oxygen by Carbon) ratios of 0.33. The presence of inherently light BC in heavy mineral fractions as well as SEM-visible mineral associations with BC particles provided evidence that the partially oxidized BC chemically interacted with the mineral phase, presumably resulting in a protection of the enclosed BC against further decomposition in soil.

Ural (2005) obtained Afsin–Elbistan (AE) by burning coal samples from top, middle and bottom sections of the AE coal seam and compared their properties. After performing

chemical analysis of the AE coal fly ashes, he showed that they are mainly composed of CaO, SiO₂, Fe₂O₃ and Al₂O₃. He also carried out Quantitative X-ray diffraction (XRD) analyses using an interactive data processing system (SIROQUANT™) based on Rietveld interpretation methods. It was found that Lime is present in all the samples, ranging from 7% to 38%. Also amorphous contents of fly ashes were ranged between 19% and 25%. He also revealed that bottom section coal fly ash is very similar to Class F, while medium and top section coal fly ashes are close to Class C. But also they do not comply with any of the standard. He presented the results and showed new possibilities for AE coal fly ashes in a wide range of fields.

Sarkar (2005) carried out comprehensive characterization of fly ash from Bokaro Thermal Power Plant, Jharkhand. He analysed non-magnetic and magnetic fractions of ash in terms of their morphological, mineralogical features and physico-chemical properties and revealed that there is a striking difference in the features and properties of the coarser and finer particles. The coarser fractions of the non-magnetic component was found to contain high percentage of char and semi coked or coked carbonaceous particles. It was found that the particles of the finer fractions have more spheroidal character than the coarser ones. The nonmagnetic components contained quartz and mullite as the main mineral phases. He stated that the Ferro spheres present in these components contained crystallites with different geometrical patterns showing change in the crystallization process.

Blanco et al. (2006) carried out analysis on two fly ashes from Asturias (Spain) by wet milling and by leaching with sulfuric acid. The activated fly ashes were characterized in terms of physico-chemical characterization, granulometry, density, BET, XRD and SEM. They carried out comparative study out of several mortars, using different additions of silica fume or activated fly ash and the influence of additives on the mechanical resistance of the mortars was also studied. It was found that mortars containing activated fly ash presented higher compressive strengths. A mercury intrusion porosimetry study was carried out on cement mortars made with mineral additives such as silica fume and activated fly ashes. These porosities values of mortars showed that mineral admixtures improved mechanical resistance due to the decrease in pore size.

Goodarzi (2006) sampled fly ash from power plants that use pulverized subbituminous and bituminous feed coals and examined for their mineralogical and elemental compositions. He stated that the concentrations of As, Cd, Hg, Mo, Ni, and Pb in fly ash are related to the sulphur content of the coal. The concentrations of these elements are also greater for bag house fly ash compared to ESP fly ash for the same station. It was found the bag house fly ash from the fluidized bed had highest content of Cd, Hg, Mo, Pb, and Se indicating that CaO, for the most part, captures them. He collected the Fly ash from a station equipped with hot side ESP (Electrostatic precipitator) and observed that it had a lower concentration of Hg compared to stations equipped with cold side ESP. Finally Fly ash particles from fluidized bed coal were found to be angular and sub angular with cores of quartz and calcite.

Kutchko et al. (2006) characterized twelve Class F fly ash samples from nine PC power plants in using scanning electron microscopy (SEM) and energy dispersive spectroscopy (EDS). They analyzed both the surface and internal structure of fly ash particles and found that all of the fly ash samples were comprised mainly of amorphous alumina-silicate spheres and a smaller amount of iron-rich spheres. The majority of the iron-rich spheres were also found to have two components: iron oxide and amorphous alumina-silicate. Cross-sections clearly revealed that the iron oxide and aluminosilicate were mixed throughout the fly ash particles. Calcium was associated with oxygen, sulfur or phosphorous, not with silicon or aluminum. The calcium-rich material was distinct in both elemental composition and texture from the amorphous alumino-silicate spheres. Elemental concentrations were determined by EDS and were consistent with ICP-OES and X-ray diffraction data.

Koukoulas et al. (2006) investigated Mineralogy and geochemistry of Greek and Chinese coal fly ash. They selected samples from China and Greece and analyzed them for determining their mineralogical and chemical composition. It was found that Chinese ash contains mullite, calcite, dolomite, and main mineral phases present in coal were quartz, kaolinite, calcite, dolomite and bohemite. Similarly the mineralogical composition of the Greek fly ash includes calcite, quartz plagioclase, anhydrite, lime, portlandite, gehlenite, hematite and amorphous material. The examined Chinese fly ash is rich in Al₂O₃ (35%)

while the Greek fly ash is CaO-rich (28%). Lastly the Chinese fly ash was found to contain lower concentrations of Ni, Cr, Zn, Ba, La, Sr and B compared to the Greek fly ash. This is due to the surrounded the coal basin rocks' composition.

Nikholaos et al. (2007) investigated chemical and mineralogical composition of fly ash samples collected from different parts of a laboratory and a pilot scale CFB facility has been investigated. Sampling points were used. They used fuels such as Greek lignite, Polish coal and wood chips. They also conducted Characterization of the fly ash samples using X-ray fluorescence (XRF), inductive coupled plasma-optical emission spectrometry (ICP-OES), thermo gravimetric analysis (TGA), particle size distribution (PSD) and X-ray diffraction (XRD). It was observed that the produced fly ashes are rich in lime (CaO). Also SiO₂ along with Al₂O₃ and Fe₂O₃ was found in considerable quantities. Results were obtained by XRD and this shows that the major mineral phase of fly ash is quartz, while other minerals present were maghemite, hematite, periclase, rutile, gehlenite and anhydrite. Lastly ICP-OES analysis revealed low levels of trace elements such as As and Cr.

Koukouzas et al. (2007) carried out analysis on chemical and mineralogical composition of fly ash samples collected from different parts of a laboratory and a pilot scale CFB facility. The fabric filter and the second cyclone of the two facilities were chosen as sampling points. The fuels used were Greek lignite, Polish coal and wood chips. Chemical composition of the fly ash samples was conducted by means of X-ray fluorescence (XRF), inductive coupled plasma-optical emission spectrometry (ICP-OES), thermo gravimetric analysis (TGA), particle size distribution (PSD) and X-ray diffraction (XRD). After performing chemical analyses the produced fly ashes were found to be rich in CaO. Moreover, SiO₂ is the dominant oxide in fly ash with Al₂O₃ and Fe₂O₃ found in considerable quantities. Results obtained by XRD showed that the major mineral phase of fly ash is quartz, while other mineral phases that are occurred are magnetite, hematite, periclase, rutile, gehlenite and anhydrite. The ICP-OES analysis showed rather low levels of trace elements, especially for As and Cr, in many of the ashes included in this study compared to coal ash from fluidized bed combustion in general.

Rubio et al. (2007) obtained Carbon-enriched fractions from two coal fly ash (FA) samples. The FA came from two pulverized-coal fired power stations (Lada and Escucha, Spain) and were collected from bag house filters. Sieving was used to obtain carbon-enriched fractions, which were further subjected to two beneficiation processes: acid demineralization using HCl and HF, and oil agglomeration using soya oil–water. Yield in weight after sieving, unburned carbon content, and several physicochemical characteristics of the obtained fractions were used to compare the performance of the beneficiation methods. Low carbon concentration was obtained by sieving, particularly in the case of Escucha FA. However, after acid demineralization or oil agglomeration, fractions containing unburned carbon in a range of 63% to 68% were obtained. These fractions showed differences in mineral phase composition and distribution depending on the FA and on the beneficiation method used. The textural properties of the obtained fractions varied as a function of their carbon content and the beneficiation method used. However, no significant differences in morphology of the carbonaceous particles were found.

Xiaor et al. (2007) investigated physical–chemical characteristics of mechanically-treated circulating fluidized bed combustion (CFBC) fly ash, such as 45 µm sieve residue, granulometric distribution, water requirement, specific gravity, pH value, and mineralogical phases. It was found that the grinding process can be divided into three stages. The increase in fineness of ground CFBC fly ash is very sharp in the first stage, then slows down in the second stage, and in the last stage it becomes almost in vary. The water requirement decreases with prolonged grinding time, and slightly increases during the last stage of grinding. Ground CFBC fly ash shows a higher specific gravity due to the crushing of coarse particles and carbon particles. The pH of ground CFBC fly ash is greater than that of the original CFBC fly ash, indicating that ground samples react more rapidly with water. The mineralogical compositions remain unchanged with grinding, although the intensity of the crystalline phases decreases and the half peak width increases.

Binay et al. (2008) performed Leaching of ten elements – namely, Fe, Mn, Ca, Na, K, Cu, Cr, Zn, As and Pb – from four fly ash samples collected from four different coal-fired

thermal power plants in West Bengal, India, has been reported. The leaching conditions were selected to broadly simulate that of surface coal mines in order to estimate the usefulness of the materials for back-filling of abandoned mines and to assess the possibility of contamination of the sites by release of heavy metal ions. Sequential batch leaching consisted of four cycles each of seven days duration; the long-term leaching continued over a period of 180 days. The starting pH of the leaching solutions ranged from strongly acidic to strongly basic. The leaching pattern and its dependence on the pH as well as the solid-liquid ratio have been critically analyzed. A much higher mobility of the elements have been expectedly observed at a low pH. Less leaching is found at a high pH except for arsenic. The mobilization pattern is strongly governed by the well-known phenomenon of dissolution and re-precipitation of iron with co-precipitation of a series of elements depending upon the pH of the medium. Extraction equilibrium was reached for Ca, Fe, Na and Zn at certain pH values. A monotonic trend of release for the elements Mn, K, Cu, Pb, Cr and As persisted over the long-term leaching period of 180 days. The alkalinity or the calcium content of an ash sample greatly determines the leaching pattern if the solution pH is neutral or mildly acidic. It appears that the risk pollution of ground water as well as of surface water may not be avoidable if fly ash alone is used for mine back-filling in an environment where acid mine drainage is prominent.

Ahmaruzzaman (2009) discussed the utilization of fly ash in construction as a low-cost adsorbent for the removal of organic compounds, flue gas and metals, light weight aggregate, mine back fill, road sub-base, and zeolite synthesis. He spent considerable amount of research using fly ash for adsorption of NO_x, SO_x, organic compounds, and mercury in air, dyes and other organic compounds in waters. It was found that fly ash is a promising adsorbent for the removal of various pollutants. It was also found that fly ash has good potential for use in the construction industry. The conversion of fly ash into zeolites has many applications such as ion exchange, molecular sieves, and adsorbents. Converting fly ash into zeolites not only alleviates the disposal problem but also converts a waste material into a marketable commodity. Investigations also revealed that the unburned carbon component in fly ash plays an important role in its adsorption capacity.

Devi et al. (2010) examines the suitability of Talcher coal fly ash for stowing in the nearby underground coal mines based on their physico-chemical and mineralogical analysis. The physical properties such as bulk density, specific gravity, and particle size distribution, porosity, permeability and water holding capacity etc. have been determined. From the chemical characterization it is found that the ash samples are enriched predominantly in silica (SiO_2), alumina (Al_2O_3) and iron oxides (Fe_2O_3), along with a little amount of CaO , and fall under the Class F fly ash category. In addition, the mineral phases identified in the ash samples are Quartz, mullite, magnetite, and hematite. The particle morphological analysis revealed that the ash particles are almost spherical in shape and the bulk ash porous in nature. From the particle size and permeability point of view, pond ash may be considered a better stowing material than fly ash. Therefore, the physico-chemical and mineralogical characterization of fly ash is essential before its effective utilization as a stowing material can be assessed and to supplement the search for other applications.

Sarode et al. (2010) carried out extraction and leaching of various heavy metals like Zn, Ni, Cu, Fe, Pb, Mn, Mg, and Cd. by applying batch leach test and toxicity characteristic leaching procedure (TCLP) for checking the possibility of ground water contamination. They also analyzed ground water samples in the locality of ash dumping sites for finding heavy metal concentrations and they also compared the results with Indian and WHO allowable limits. Mg, Mn, and Fe were leached to a larger degree while Zn, Cu, and Pb to moderate and Ni to a smaller extent, from the ash and admixture samples. Cd was not leached at all from any sample in batch leach as well as TCLP tests. The concentrations of Zn, Fe, Mn, Mg, and Cd in groundwater samples were below the permissible limits of WHO and Indian standards. The concentrations of Ni and Pb were slightly higher than WHO permissible limits but below the Indian standards. The concentration of Cu was within the WHO permissible limits but slightly higher than Indian Standards.

Bhattacharjee et al. (2011) studied the physical nature of the fly ash sample of the Kolaghat Thermal Power Plant, India. They estimated particle sizes of this fly ash sample from the SEM images and observed that it lied within 0.16–5.50 mm. Similarly EDX spectral analysis performed indicated the presence of O, Al, Si, C, Fe, Mg, Na, K and Ti in

this sample. From the XRD analysis, it was found that physical nature of fly ash is crystalline and the major components are mullite ($\text{Al}_6\text{Si}_2\text{O}_{13}$) and quartz (SiO_2). Also, the presence of hematite, microcline, magnetite, magnetite and free iron in smaller fractions were detected. They noticed large magnetization at 5 K which showed the presence of magnetic components. In general, XRD analysis provides the quantitative estimation of the different iron ions present in the sample. Precisely, they presented experimental data on physical aspects of the fly ash sample of a thermal power plant and deals with an in-depth analysis of it.

Chengu et al. (2011) investigated the effects of coal fly ash size, sulfuric acid concentration, and reaction time and reaction temperature on extraction efficiency of aluminum. They analyzed phase and morphology of coal fly ash and solid residues after reaction using XRD, SEM and IR. It was confirmed that optimum conditions for extracting aluminum from coal fly ash with size of 74 μm and sulfuric acid with concentration of 50% are mixed in pressure reaction kettle to react for 4 h at 180 °C. Under the optimal conditions, the extraction efficiency of aluminum can reach 82.4%.

Nally et al. (2012) obtained fly ash from power plant in Pennsylvania and tested for its leaching potential of selected trace metals such as Al, As, Ba, Ca, Cr, Co, Cu, Fe, Pb, Mg, Mn, Ni, Se, Sr, V, and Zn). They confirmed SEM observations that fly ash has an abundance of large, porous, irregular shaped grains that would absorb water, which adversely affect the quality of a cement application. They also compared with another fly ash. They also showed typical glass spheres demonstrating the differences in fly ash structure and its physical characteristics. An analysis of FA performed depicted total metal content and also indicated a number of trace metals over the cleanup standard limits for residential land over an aquifer. The fly ash leaching potential was determined by the Toxicity Characteristic Leaching Procedure (TCLP) and the Synthetic Precipitate Leaching Procedure (SPLP) tests. The results show that Se was over the TCLP limit, while As and V were over the U.S. drinking water Maximum Contaminant Level (MLC) for the SPLP test.

Three ash samples S-I, S-II and S-III were collected from Bhatinda thermal plant, Hisar thermal plant and Ropar thermal plant, respectively. The various characterization or morphological studies that were done on the three Fly and Bottom ash samples included Particle size distribution, scanning electron microscopy (SEM) analysis, energy dispersive X-ray spectroscopy (EDS) analysis XRD (X-ray diffraction) and DTA (Differential Thermal analysis). Particle size distribution graphs were generated for three Fly and Bottom ash samples in order to find the percentage of finer particles and mass median diameter of these samples.

3.1 PARTICLE SIZE DISTRIBUTION

It is defined as the measurement of the size of the particles contained in a batch of material and their distribution in proportion to their size. PSD is very crucial for understanding physical and chemical properties of a fly and Bottom ash. We applied Sieve analysis as the basis for comparing the fineness of these 3 types of fly ash (S-I, S-II and S-III). Both the finer material and the material retained in Sieves were dried in Oven. The Dried ash material is passed through number of Sieves consisting of mesh of various sizes. Meanwhile each ash sample was sieved for 30 min in a sieve shaker using sieves no. 8, 10, 16, 22, 30, 44, 60, 100, 150, 200 and 300. The sample retained on each sieve is collected and each of the size fractions so obtained was separately analyzed for particle size distribution and the percentage retained on each sieve is calculated using the standard procedure to obtain the sieve curve. Following Diagram shows the Sieve analysis machine in our workshop. In this experiment particle size varies from 2000 μm to 53 μm .



Fig 3.1 Sieve analysis machine

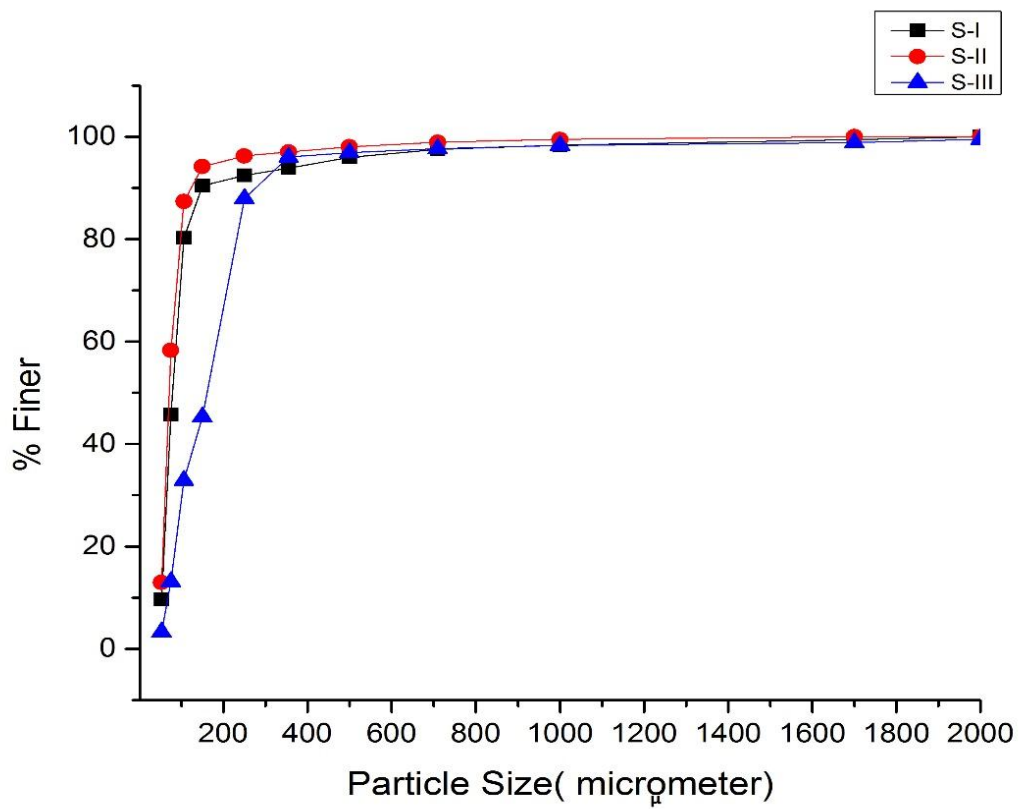


Fig. 3.2 Particle size distribution graph for 3 samples of fly ash

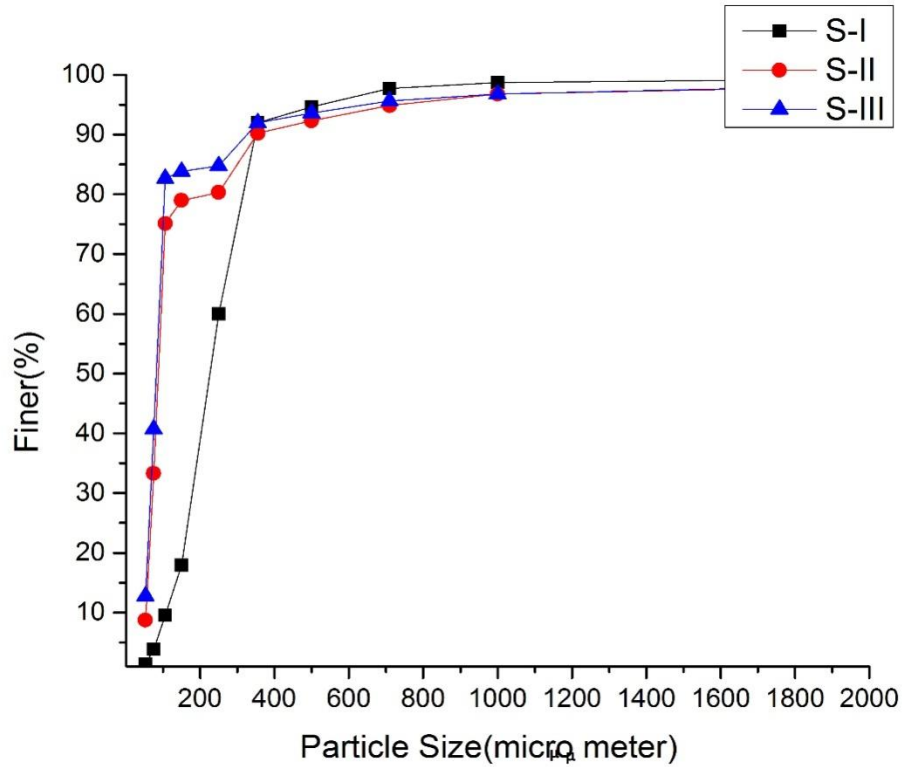


Fig. 3.3 Particle size distribution graph for 3 samples of bottom ash

From Fig. 3.2-3.3 in case of fly ash, S-I sample is finer than other fly ash samples and in case of bottom ash, S-I sample is finer than other bottom ash samples. This is because 12.94% of S-I fly ash particles are finer than 53 μ m.

3.2 SEM (SCANNING ELECTRON MICROSCOPY) ANALYSIS

Scanning Electron Microscopy was done in order to analyze Morphological and texture properties of ash samples. The signals produced from electron-sample interactions provides information about the sample including external morphology, chemical composition, crystalline structure and orientation of materials constituting the sample. These electrons act with the atoms in the sample, producing various signals that contain information about the sample's surface configuration and composition. The equipment used was SEM-JSM-6510LV JEOL. The SEM micrographs that were obtained for three samples S-I, S-II and S-III (2000X) without leaching are shown in Fig 3.4 -3.6 and Fig 3.7-3.10.

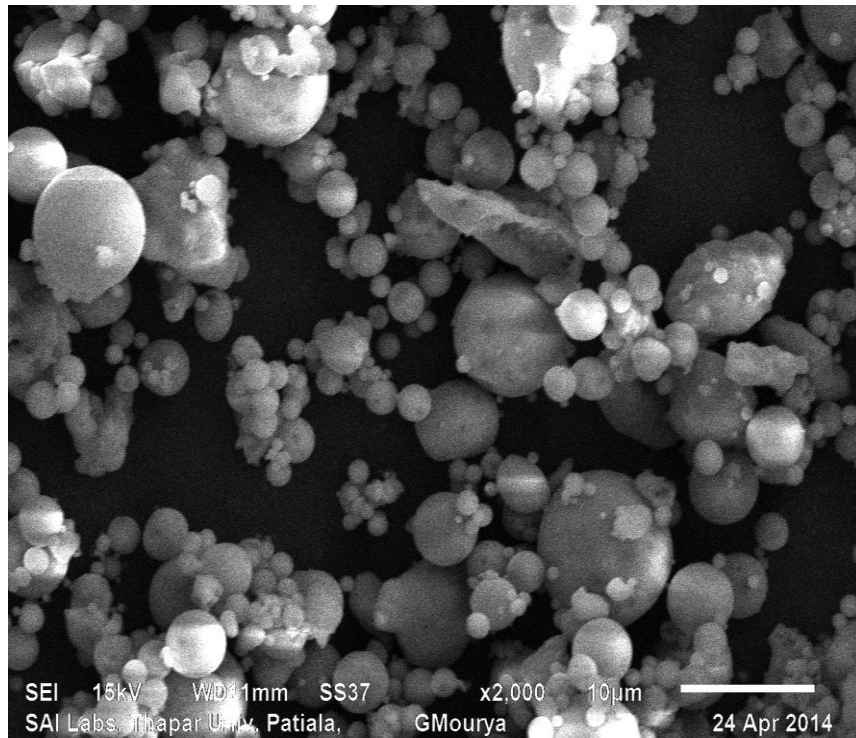


Fig.3.4 SEM image of S-III fly ash (at 2000X)

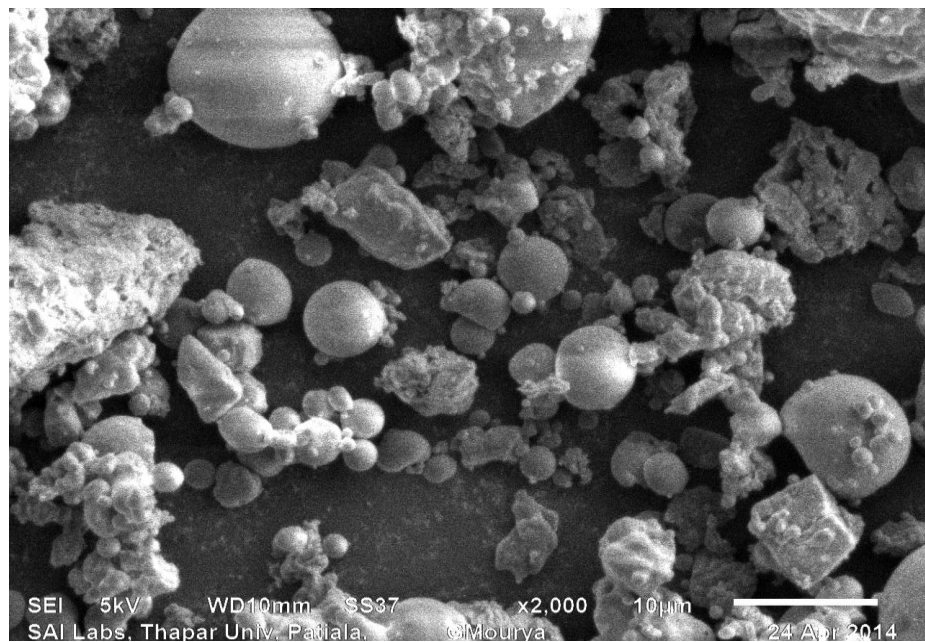


Fig. 3.5 SEM image of S-I fly ash (at 2000X)

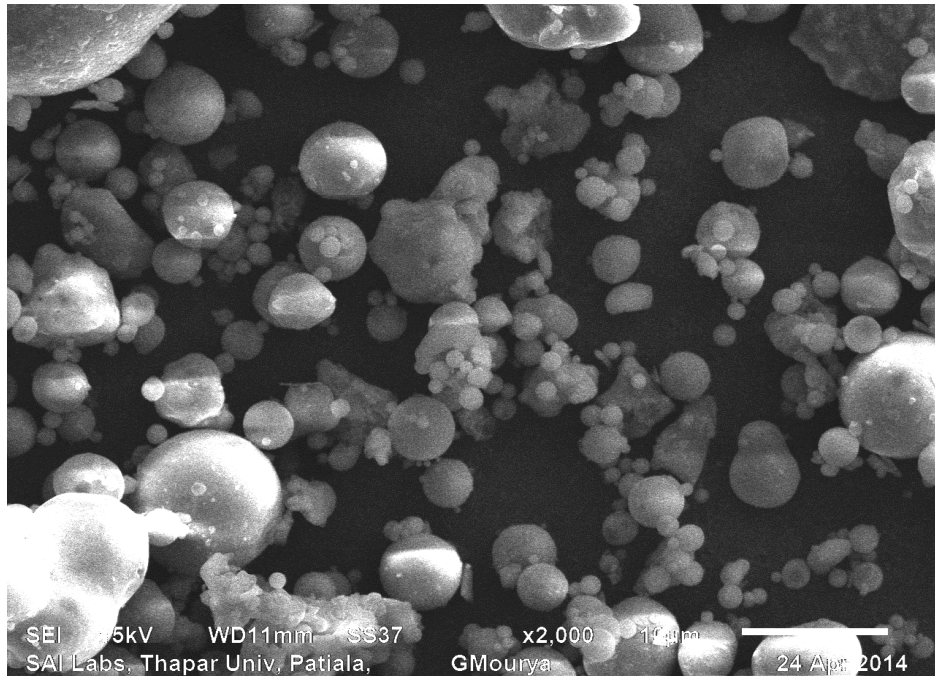


Fig. 3.6 SEM image of S-II fly ash (at 2000X)

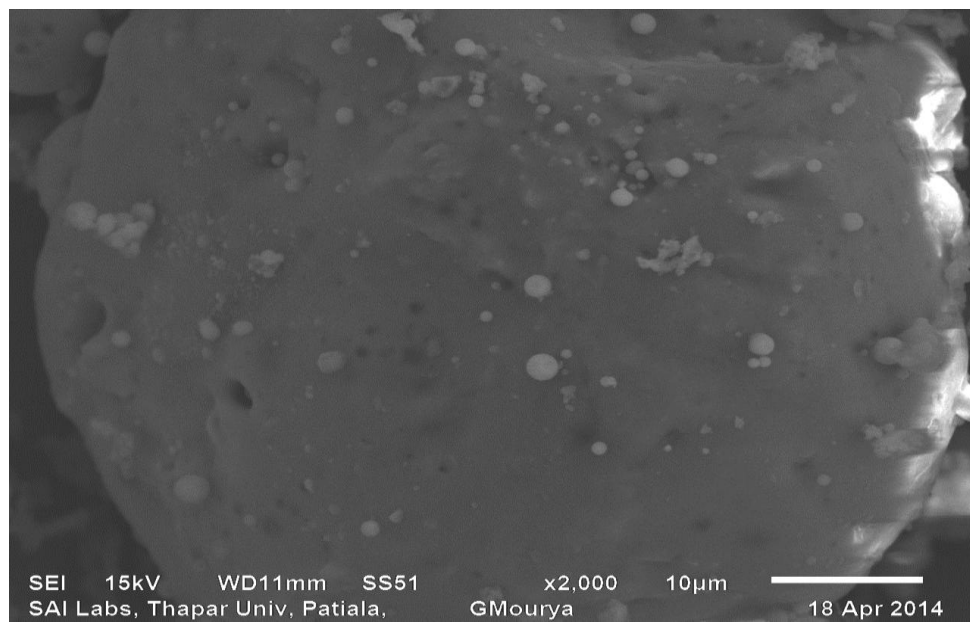


Fig. 3.7 SEM image of S-III bottom ash (at 2000X)

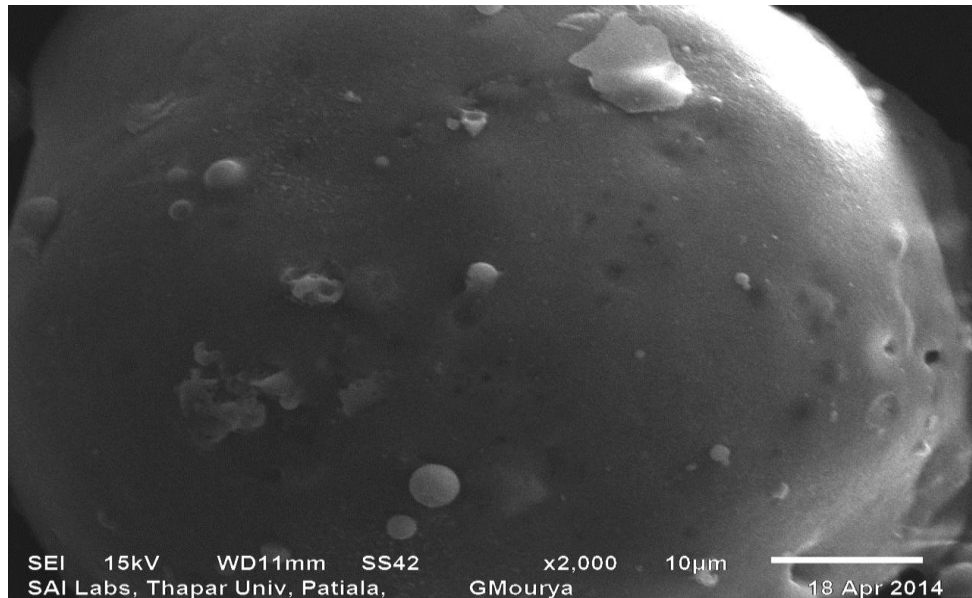


Fig. 3.8 SEM image of S-I bottom ash (at 2000X)

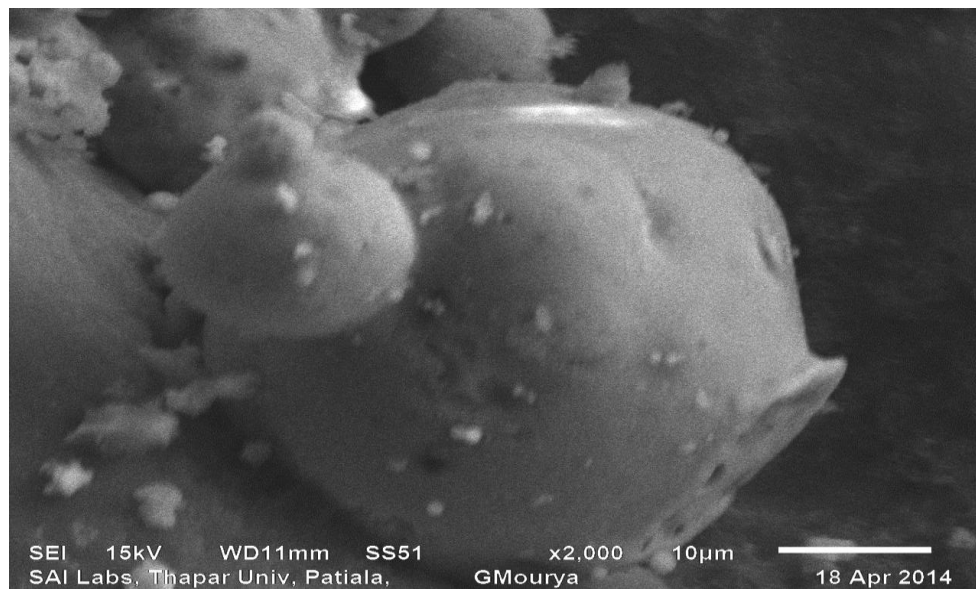


Fig. 3.9 SEM image of S-II bottom ash (at 2000X)

The observations from the SEM analysis conducted on the Fly ash samples showed that all the Fly ash samples contained particles that were mostly Spherical in shape (in case of S-III and S-II Fly ash) along with aggregates of hollow spheres (Cenospheres). Particles of

irregular shape such as disturbed spheres as well as aggregates were observed in S-I fly ash sample. These samples mainly consisted of aluminosilicate glassy spheres, angular quartz, and occasionally mullite spheres were also identified. The micrograph of S-I fly ash sample depicted a mixture of coarse and fine spherical particles. In case of bottom ash, S-III and S-I samples consists mostly heavier and Spherical Particles consisting of lesser aggregates. S-II bottom ash contained mostly irregular shape aggregates and lesser spherical particles.

3.3 ENERGY DISPERSIVE X-RAY SPECTROSCOPY (EDS) ANALYSIS

EDS is an analytical technique used for the elemental or chemical analysis of a sample. It makes use of some interaction of some source of X-ray excitation and a sample. It is based on the fact that each element has a unique atomic structure thus allowing unique set of various peaks on its X-ray spectrum. For stimulating the emission of characteristic X-rays from a specimen, a high-energy beam of charged particles such as electrons or protons or a beam of X-rays, is focused on the sample being studied. At rest, an atom within the sample contains ground state (or unexcited) electrons in discrete energy levels or electron shells bound to the nucleus. The incident beam excites an electron in an inner shell, ejecting it from the shell while creating an electron hole where the electron was. In this process some radiations are released when electron moves from lower shell to higher shell this difference in energy between the higher-energy shell and the lower energy shell is expelled in the form of an X-ray. The number and energy of the X-rays emitted from a specimen is measured by an energy-dispersive spectrometer. As the energy of the X-rays are characteristic of the difference in energy between the two shells, and of the atomic structure of the element from which they were emitted, this allows the elemental composition of the specimen to be measured. Also, images produced by electrons processed from the sample reveal surface topography or mean atomic number differences according to the mode selected. The EDS spectrums that were obtained for three different Fly and bottom ash samples are shown in the following Fig.3.10 - 3.15.

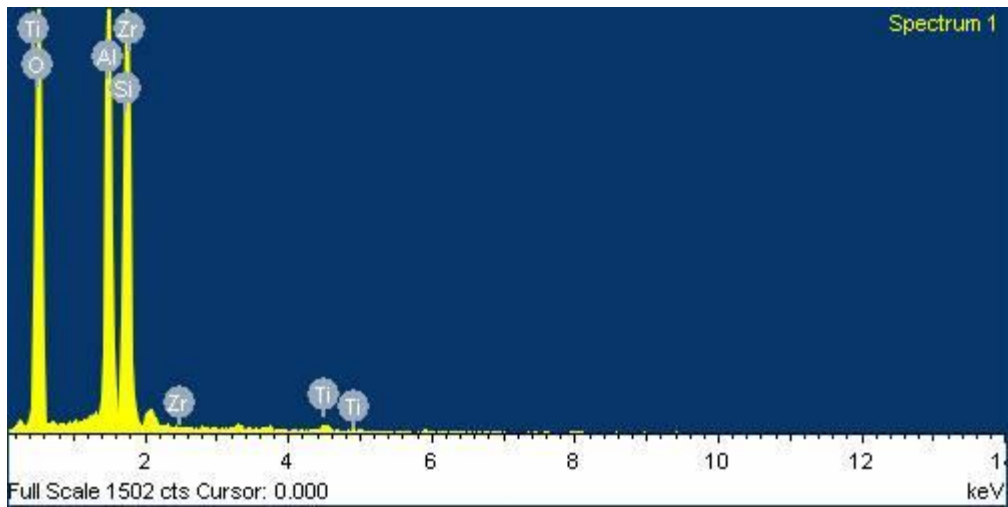


Fig. 3.10 EDS spectrum of S-III Fly Ash

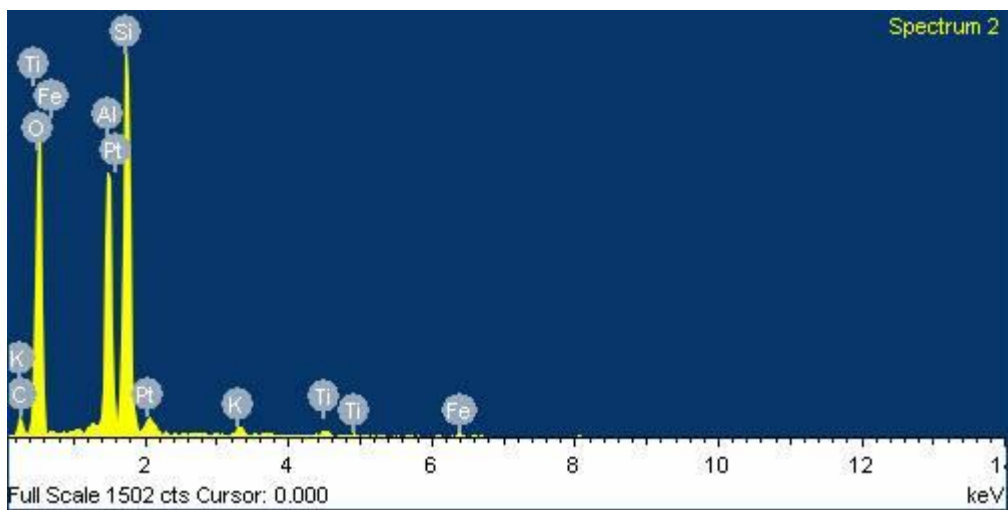


Fig.3.11 EDS spectrum of S-I Fly Ash

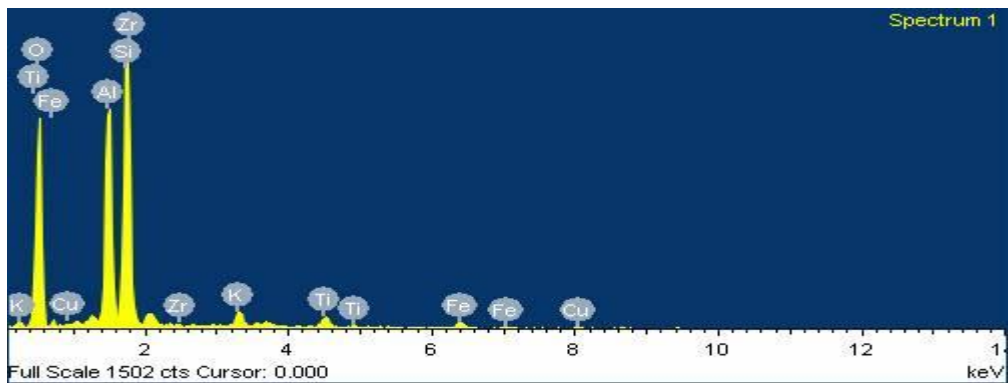


Fig. 3.12 EDS spectrum of S-II Fly Ash

From Fig. 3.10 to 3.12 it was found for all three Fly ash samples(S-I, S-II and S-III), the peaks in the EDS spectrum were corresponding to Silicon, Aluminum and Titanium. This shows that in all three samples these elements were present in great proportions. Other elements included were Copper, Potassium, and Zirconium.

The Composition of all these three samples of Fly ash are given below in tables 3.1.

Table 3.1 Composition of fly ash samples

Elements	S-III (% Weight)	S-I (% Weight)	S-II(% Weight)
O	62.54	57.23	55.41
Al	15.74	12.01	14.09
Ti	0.45	0.56	1.47
Si	19.31	20.69	22.14
Zr	1.96	-	2.91
C	-	5.71	-
K	-	0.55	1.54
Pt	-	2.58	-
Fe	-	0.67	1.42
Cu	-	-	1.02

From Table 3.1 we can see that Aluminum, Oxygen and Silicon were mostly present in these Fly ash samples. Those present in minor proportions were Titanium, Copper, Zirconium, Platinum and Carbon.

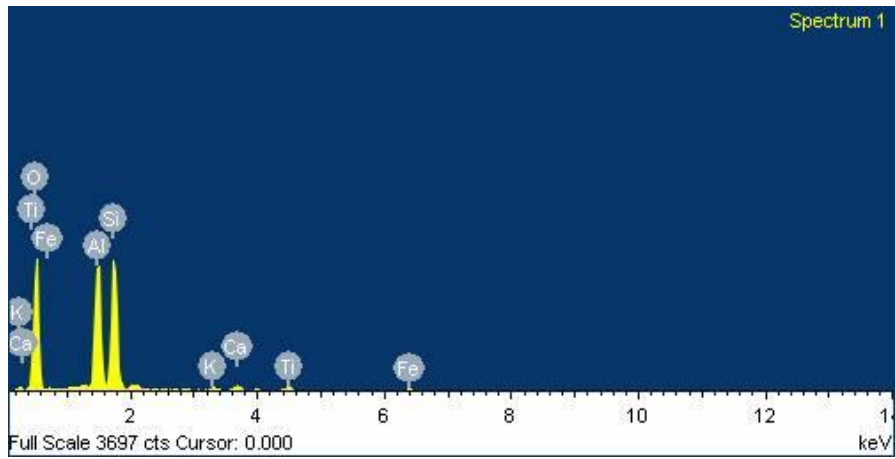


Fig.3.13 EDS spectrum of S-III Bottom Ash

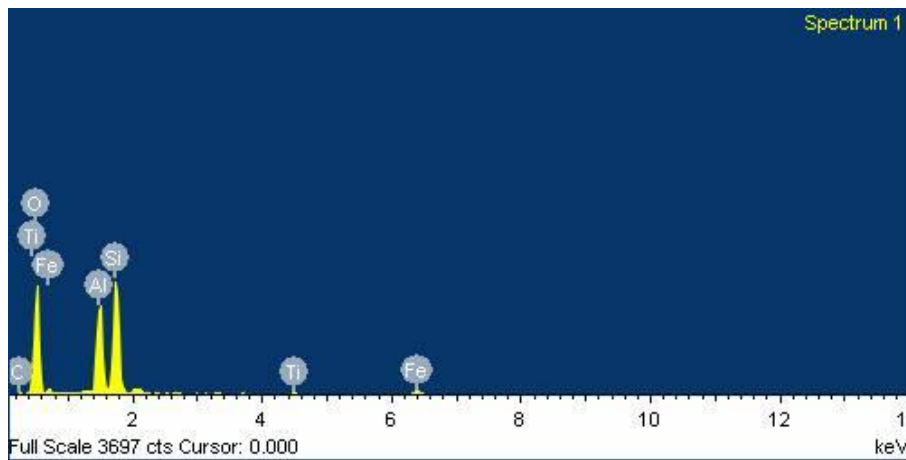


Fig. 3.14 EDS spectrum of S-I Bottom ash

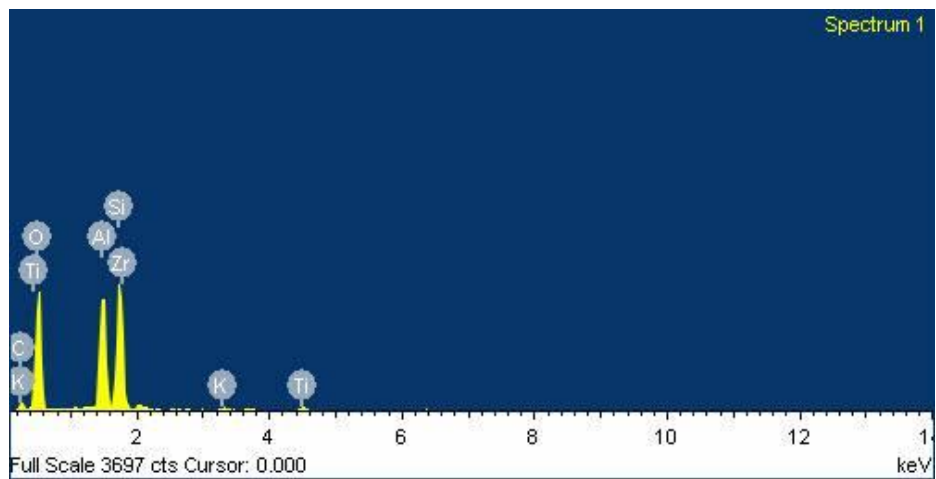


Fig. 3.15 EDS spectrum of S-II Bottom ash

From Fig 3.13 to 3.15 it was found for all three Fly ash samples, the peaks in the EDS spectrum were corresponding to Silicon, Aluminum and Titanium. This shows that in all three samples these elements were present in great proportions. Other elements included were Copper, Potassium, and Zirconium.

The Composition of all these three samples are given below in tables 3.9 -3.11.

Table 3.2 Composition of samples (Bottom ash)

Element	S-III (%Weight)	S-I(%Weight)	S-II(%Weight)
Oxygen	60.57	58.61	56.28
Aluminum	15.53	12.56	11.53
Silicon	20.38	19.65	15.37
Potassium	0.55	-	0.42
Calcium	1.01	-	-
Titanium	0.99	0.56	0.88
Iron	0.97	2.57	-
Carbon		6.05	13.82
Zirconium			1.70

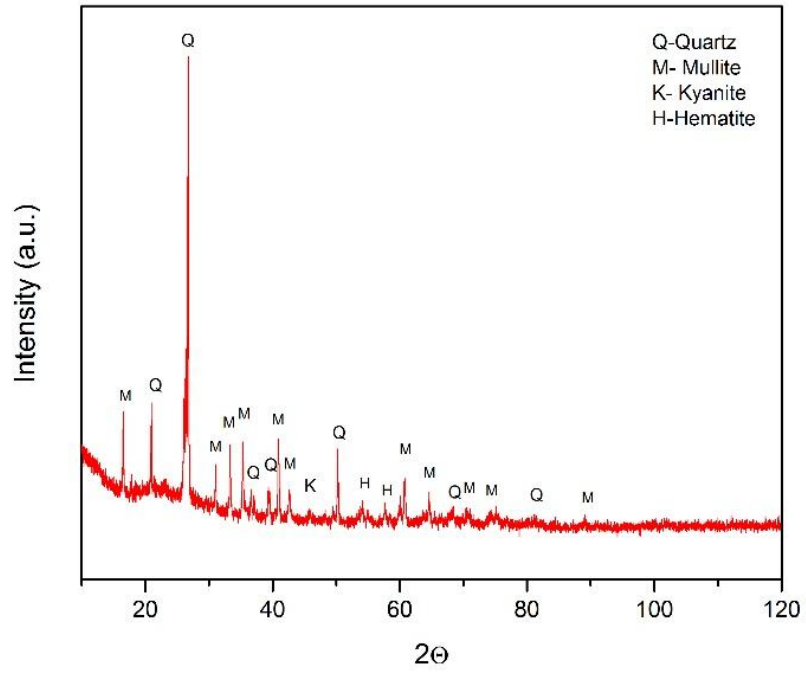
From the Table 3.2, it was found that all the three Bottom ash samples(S-I, S-II and S-III) contained Aluminum, Silicon and Oxygen in greater proportions. Apart from these elements, the other elements those were present in minor proportions included Iron, Calcium, Zirconium and Carbon.

3.4 MINEROLOGICAL PROPERTIES OF COAL ASH

Mineralogical studies include XRD (X-ray powder diffraction) and DTA (Differential Thermal analysis). These Experiments have been performed on S-I, S-II and S-III Fly and Bottom ash samples obtained from different Thermal power plants of Punjab and Haryana. XRD analysis revealed Quartz and mullite as main components whereas DTA/TG analysis revealed Thermal properties such as Melting point, Moisture Content etc. of fly and bottom ash at various temperatures. XRD ANALYSIS is a rapid analytical technique primarily used for phase identification of a crystalline material and can provide information on unit cell dimensions. X-ray diffraction is now a common technique for the study of crystal structures and atomic spacing.

X-ray diffraction is based on constructive interference of monochromatic X-rays and a crystalline sample. These X-rays are generated by a cathode ray tube, filtered to produce monochromatic radiation, collimated to concentrate, and directed toward the sample. The interaction of the incident rays with the sample produces constructive interference and a diffracted ray when conditions satisfy Bragg's Law ($n\lambda=2d \sin \theta$), where d is the spacing between the layers. These diffracted X-rays are then detected, processed and counted. By scanning the sample through a range of 2θ (Bragg angles), all possible diffraction directions of the lattice should be attained due to the random orientation of the powdered material.

XRD analysis was conducted on samples of fly ash S-I, S-II and S-III from the results of the analysis are shown below starting with the S-II sample. The JCPDS data files have been used for matching the identification of the minerals present in the Ropar Fly Ash sample. From the result we can infer that Quartz is the mostly prevalent element present in the S-II sample. Other elements include Hematite, Kyanite and Mullite. Following XRD peaks of fly and bottom ash samples have been shown in the graphs from Fig.3.16 to Fig.3.21.

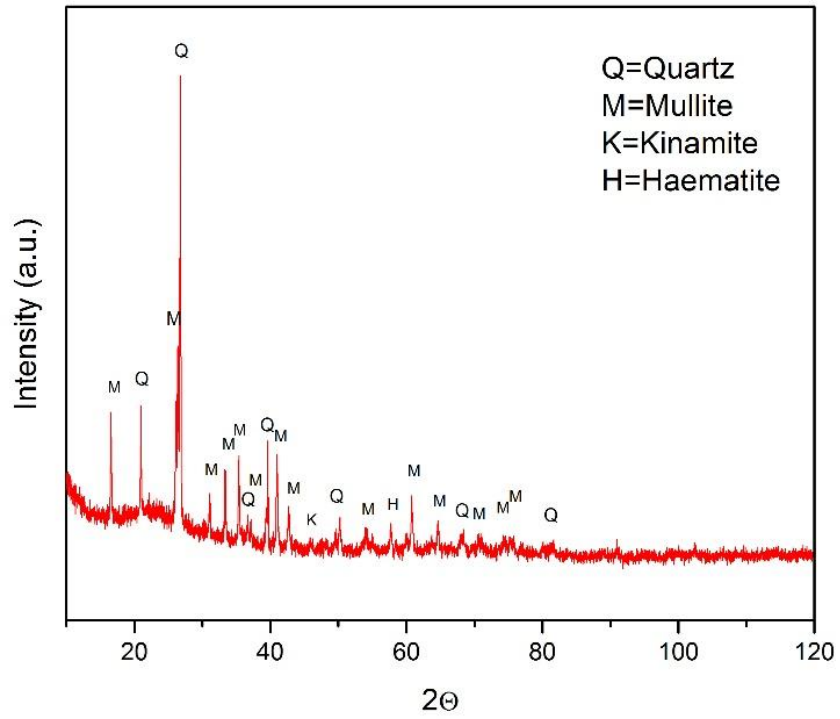


2θ → Bragg angle

Fig. 3.16 XRD peaks of S-II Fly ash

Table 3.3 Minerological Composition of S-II Fly ash

Mineral	Composition
Quartz	48.05%
Mullite	43.07%
Hematite	5.4%
Kinamite	3.3%



2θ → Bragg angle

Fig: 3.17 XRD peaks of S-III Fly ash

Table 3.4 Mineralogical Composition of S-III Fly ash

Mineral	Composition
Quartz	49.4%
Mullite	13%
Hematite	0.1%
Kinamite	37.5%

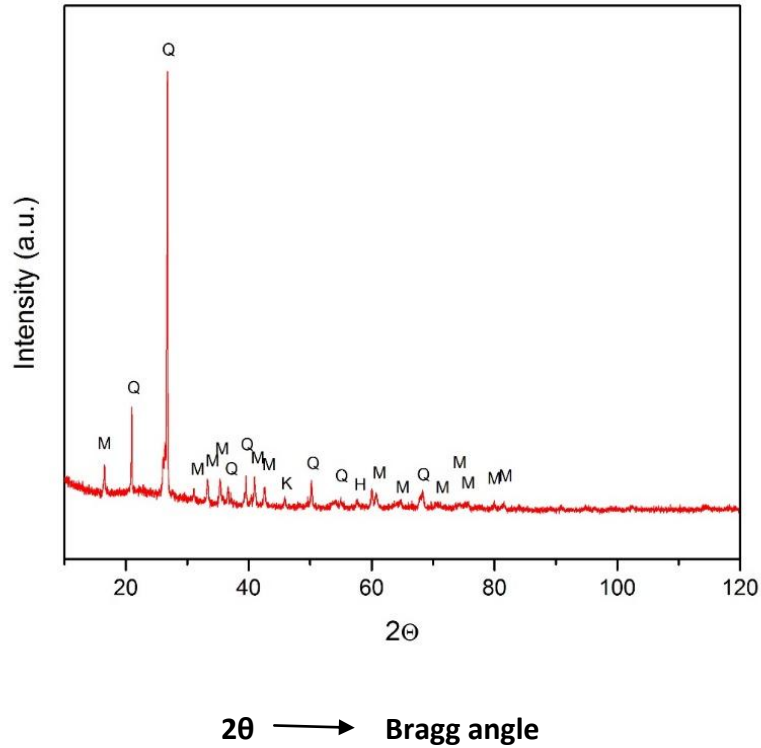


Fig: 3.18 XRD peaks of S-I fly ash

Table: 3.5 Mineralogical composition of S-I fly ash

Mineral	Composition
Quartz	63.14%
Mullite	33.6%
Kinamite	1.9%
Haematite	1.8%

Thus from the above graphs it is seen that Quartz and Mullite dominates the list of minerals indexed from the three samples of Fly ash(S-I, S-II and S-III). Other Elements such as Kinamite and Hematite are also present in trace amounts.

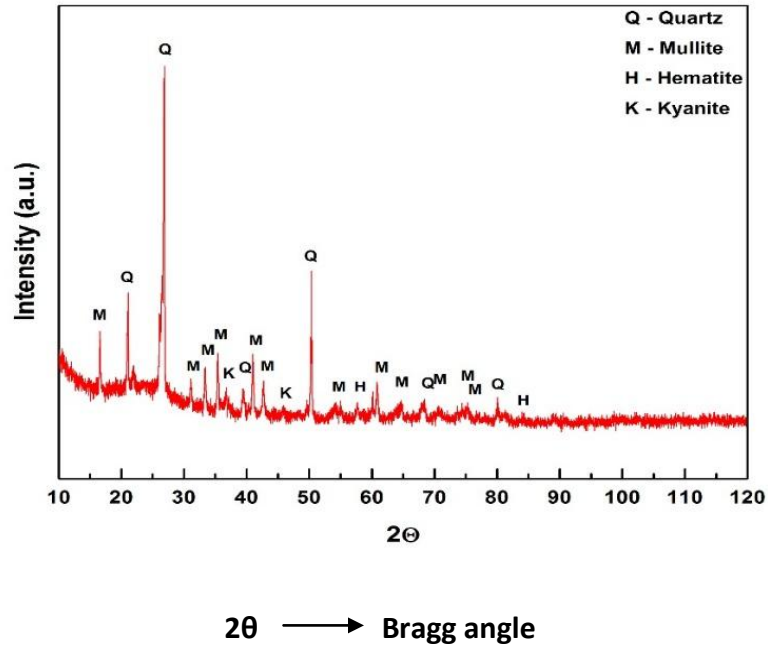


Fig.3.19 XRD peaks of S-II bottom ash

Table 3.6 Mineralogical composition of S-II bottom ash

Mineral	Composition
Quartz	46.8%
Mullite	43.4%
Hematite	4.2%
Kinamite	5.6%

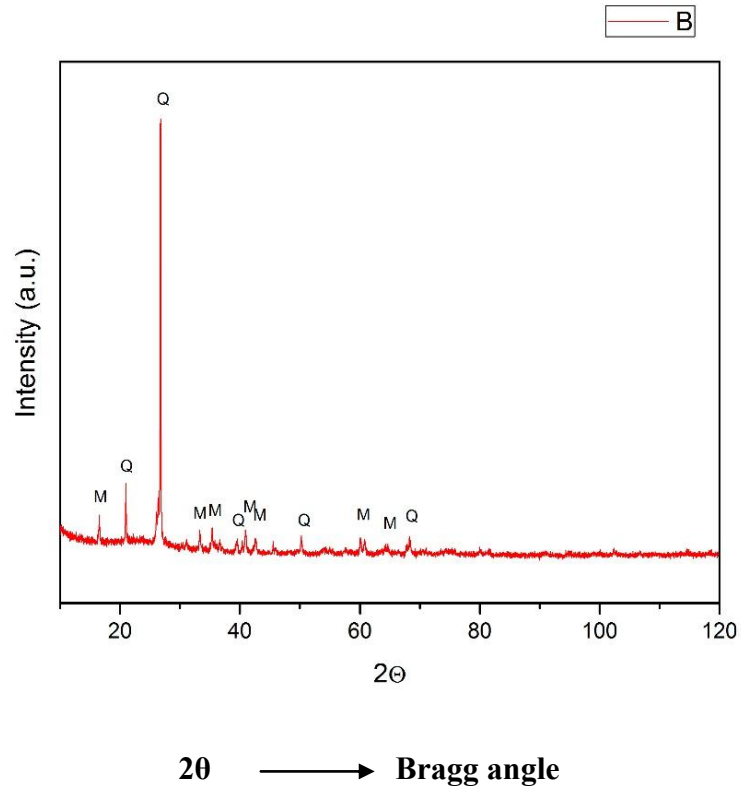
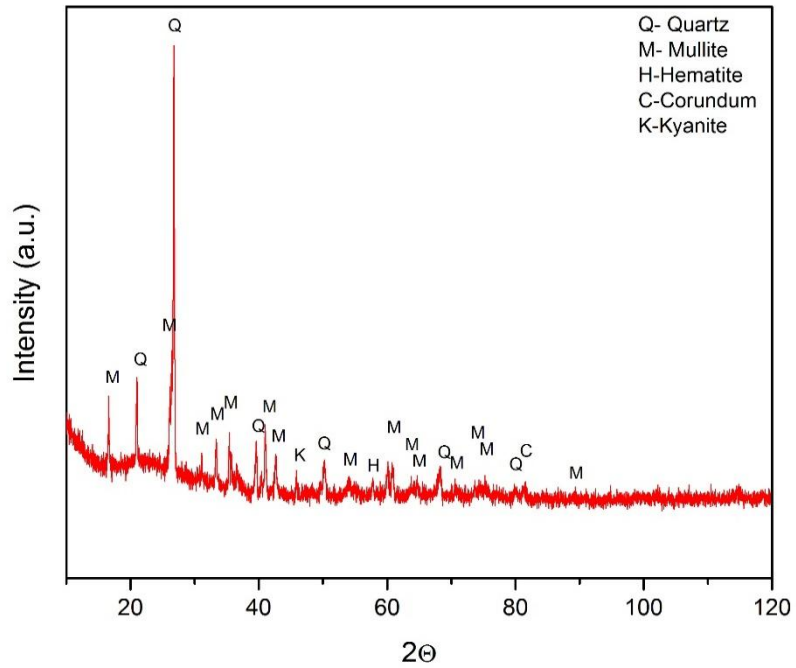


Fig 3.20 XRD peaks of S-III Bottom Ash

Table 3.7 Mineralogical composition of S-III bottom ash

Element	Composition
Quartz	71%
Mullite	29%



2θ → Bragg angle

Fig 3.21 XRD peaks of S-I Bottom Ash

Table 3.8 Mineralogical composition of S-I bottom ash

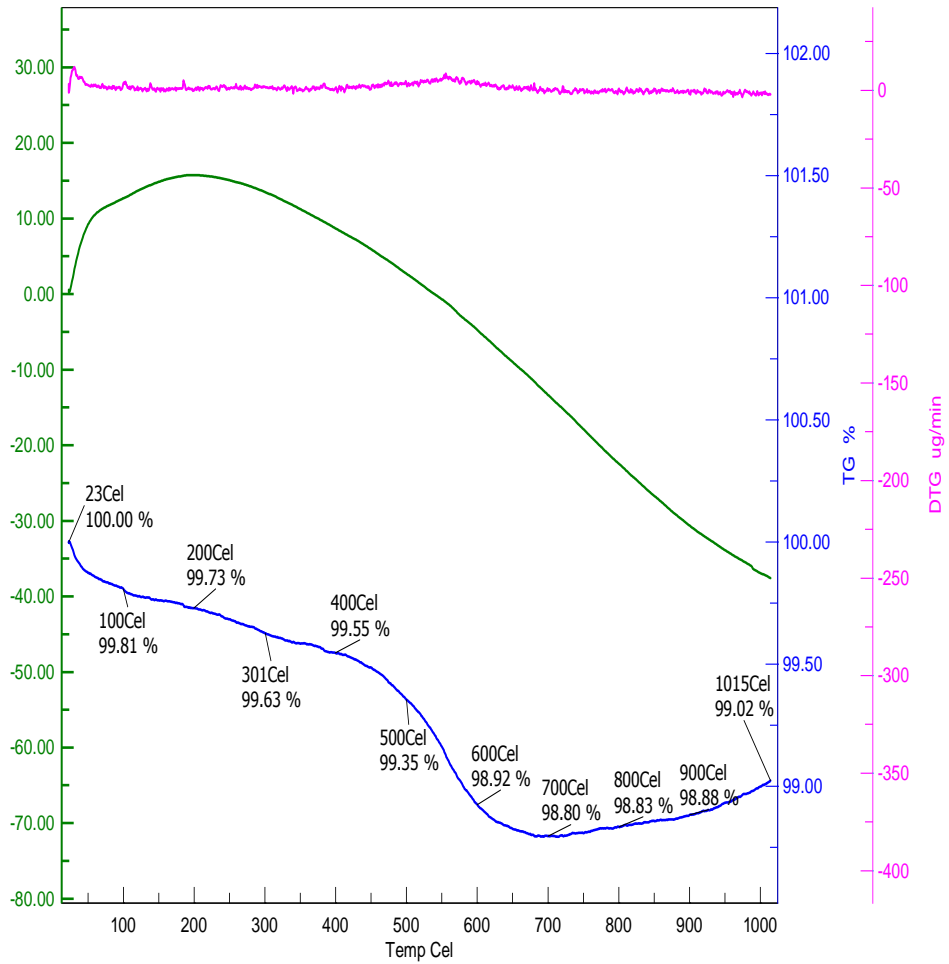
Element	Composition
Quartz	40.5%
Mullite	53.9%
Hematite	2.5%
Corundum	2.9%

3.5 THERMAL ANALYSIS OF COAL ASH

Three different Indian Fly and Bottom ash samples (in raw form) each varying in ash and moisture contents, were collected from different thermal power plants. In this chapter DTA analysis have been performed on three fly ash samples (S-I, S-II and S-III). Below are the curves which indicate the DTA/TG graphs of these samples. Thermal Analysis (TA) is defined as group of techniques that study the properties of materials which change with temperature.

Thermal analysis gives in depth information on properties like enthalpy, mass change and the coefficient of heat expansion. Differential thermal analysis is defined as the technique in which difference in temperature (dT) between a sample and a reference material is measured when they are exposed to a controlled temperature conditions. In this analysis we have taken 10.5 mg of sample (s) and inert reference (r). These are contained in Aluminum pans each with thermocouple, held in heating block, with thermocouple.

Both sample and reference material must be heated under carefully controlled circumstances. If the sample undergoes a physical reaction or a chemical reaction, its temperature will change while the temperature of the reference material remains the same. That is because physical changes in a material such as phase changes and chemical reactions usually involve changes in the heat content of the material. The differential temperature thus found is plotted against time which is known as DTA curve and if difference in temperature is plotted against temperature then it is known as Thermo gram. Changes may be physical or chemical depending on the characteristics of the material being used as sample. Following figures from 3.22 to 3.27 illustrate the DTA/TG graphs of both Bottom and Fly ash samples(S-I,S-II and S-III).



— DTA — TG — DTG

Fig 3.22 DTA/TG graph of S-III fly ash

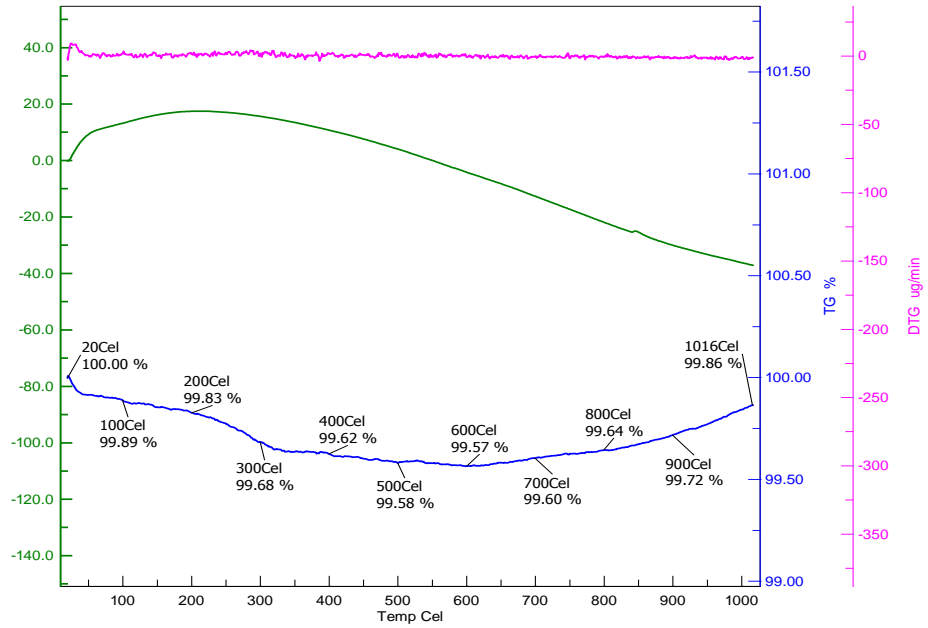
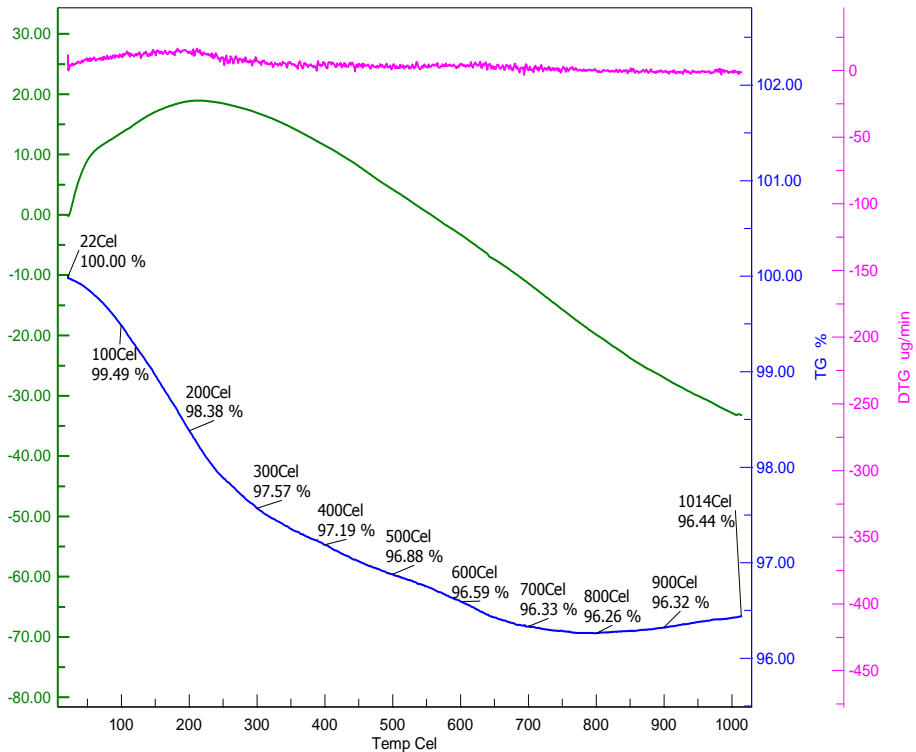


Fig 3.23 DTA/TG graph of S-I Fly Ash



— DTA — DTG — TG

Fig 3.24 DTA /TG graph of S-II Fly Ash

DTA/TG GRAPH (S-III FLY ASH)

DTA Curve tells about the melting point of fly ash and Glass transition temperature. As the heating starts at 32⁰C, Glass transition of fly ash takes place and as the curve reaches its peak, Crystallization takes place which converts amorphous forms of mullite and quartz present in ash into crystalline form known as zeolites. Maximum glass content corresponds to a peak at 250⁰C (Exothermic reaction). Melting point is 230⁰C. Also the endothermic peak is located at 700⁰C which is due to the decomposition of Calcium Hydroxide present in fly ash. The calcium hydroxide content is good indicator of pozzolanic reaction. Thus from DTA alone it is possible to assess the pozzolanic properties of S-III Fly ash. Cumulative weight loss was plotted against temperature. In this graph plotted weight loss is related to loss due to dehydration as the temperature progresses.

Looking from the TG graph we came to know about water presence in S-III fly ash. Now as the the curve progresses with increase in temperature, there comes a point at 500⁰C in which slope decreases till temperature reaches at 700⁰C. This shows more loss of water occurs in this region. Thus at temperature range between 400⁰C and 700⁰C most hydrates such as Calcium hydroxide present in fly ash undergo dehydration. Total removal of moisture occurs in the range of 500⁰C to 700⁰C. Beyond 700⁰C dehydration process completes. At 750⁰C complete destruction of crystalline lattice occurs and about 950⁰C crystallization of new phase occurs. The residue left at higher temperature (1020⁰C) indicates the presence of oxides mainly those of silicon, aluminum, Zirconium which are stable at higher temperatures. Beyond 700⁰C there is less dehydration. This may be due to less porosity of fly ash at higher temperatures. The first weight loss was observed between 100⁰C and 400⁰C which corresponds to removal of physically adsorbed water and light volatiles with loss of 0.65%. The second weight loss between 400⁰C to 700⁰C shows the active pyrolysis and oxidation with loss of 1.05%. Melting point is 500⁰C. DTG graphs indicates there is no active pyrolysis and oxidation degradation of the components of fly ash sample and weight loss occurs only in first step after that weight loss is nearly constant per unit minute.

DTA/TG GRAPH (S-I FLY ASH)

Slope inclination is less compared to S-III fly ash indicating less rate of crystallization of alumina-silicates compared to S-III sample which are mostly present in this sample. Before onset of crystallization takes place, at 32°C glass transition of cenospheres takes place. Endothermic peak is located at 600°C indicating the completion of decomposition of hydrates of potassium and iron. Melting point is 200°C. In case of S-I Fly Ash, Curve is more or less continuous with less no of bumps indicating less dehydration rate which says about low moisture content of this sample. Ash with low moisture content improves workability, increases strength of cement when added to it and possibly increases time of settling. Thus S-I Fly ash is preferable to S-III Fly Ash economically. Nearly same as that of S-III fly ash with very fewer no of peaks meaning no weight loss (due to oxidation or reduction) per degree increase in temperature.

DTA/TG GRAPH (S-II FLY ASH)

From the graph we see that slope is highest for DTA curve of S-II Fly ash which indicates rate of crystallization is highest among three fly ash samples. Endothermic peak of Ropar fly ash is at 800°C which indicates that decomposition of hydrates present in ropar fly ash completes. Melting point is 230°C almost same as that of other samples. Graph shows that downslope of TG curve is higher than S-I and S-III samples indicating larger degree of water loss implying that Ropar fly ash has more moisture content than other two samples. Therefore it is less suitable from industrial and economic point of view. Complete decomposition of hydrates stops at 800°C. Water loss rate is 3.56%.

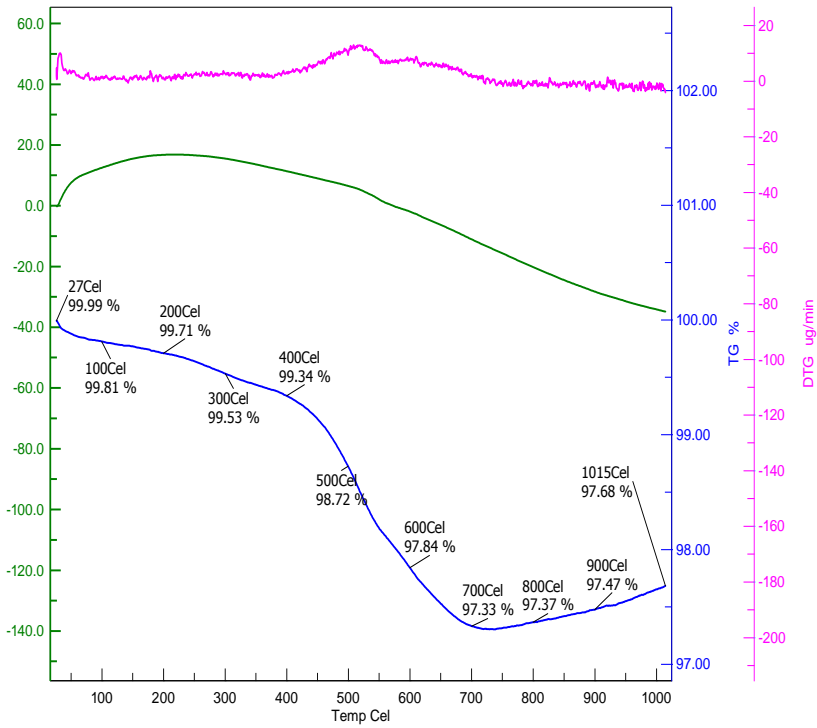


Fig 3.25 DTA/TG graph of S-III bottom ash

— DTA — DTG — TG

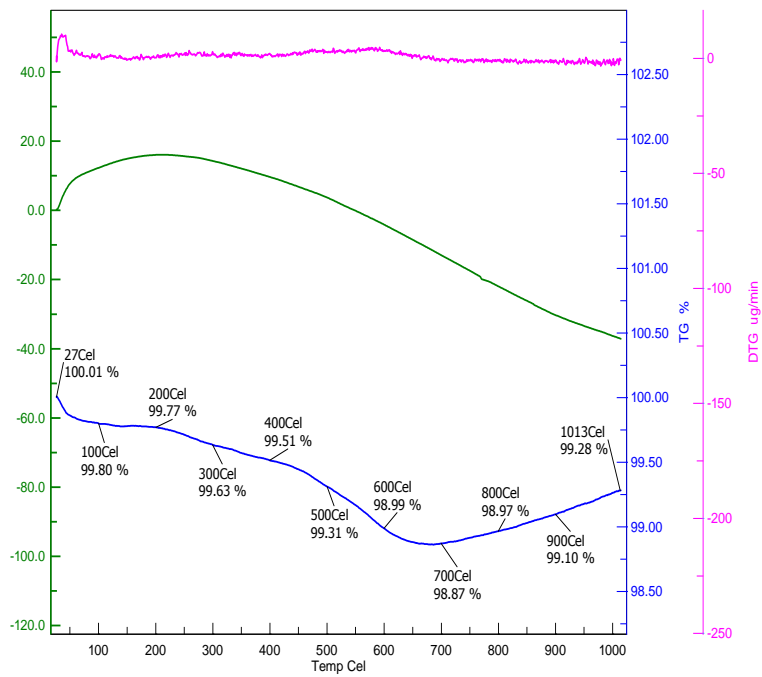


Fig 3.26 DTA /TG GRAPH OF S-I BOTTOM ASH

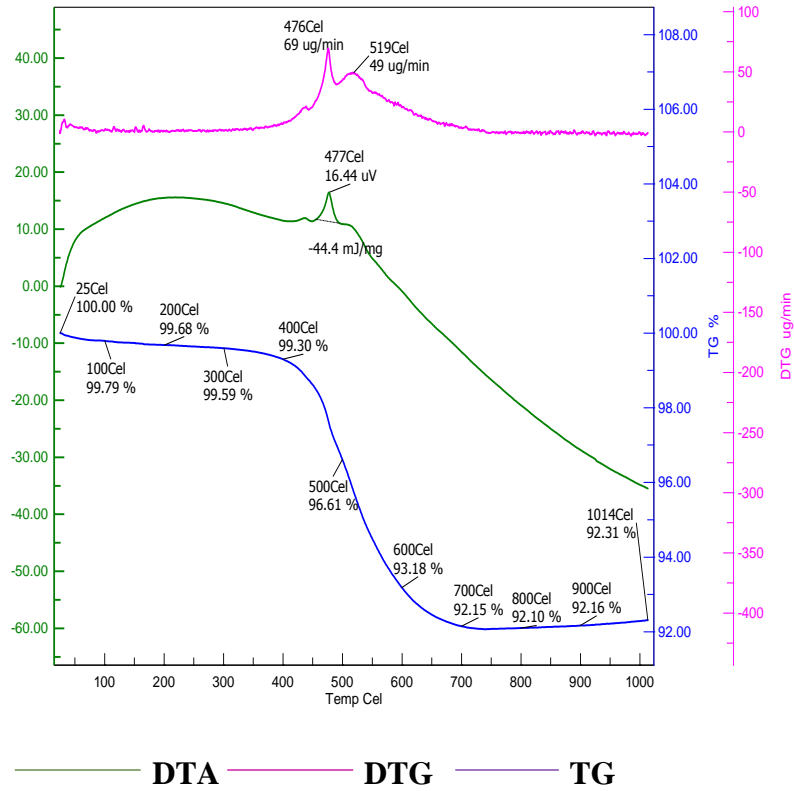


Fig 3.27 DTA /TG graph of S-III bottom ash

DTA CURVE (S-I, S-II and S-III bottom as samples)

It shows the peak which indicates that oxidation or reduction of elements takes place releasing energy at the rate of -44.4 mJ/mg. Negative sign indicates exothermic reaction takes place. Steep curve of DTA indicates larger degree of decomposition of hydrates present. Melting point is same as that of fly ash samples (250°C). S-III bottom ash follows up in the rate of dehydration (2.31%) whereas S-I Bottom ash encounters less degree of dehydration (0.72%).

TG CURVE

This curveshows much larger degree of water loss among all samples of Fly and Bottom ash. Water loss rate is 7.69%. At temperatures of about 700°C all moisture content is removed thus decomposition of hydrates is ceased.

DTG CURVE

In case of S-III and S-II Bottom ash shows peaks indicating degree of mass loss per minute due to oxidation or reduction while Hisar shows no peaks .This is due to presence of Calcium and Potassium hydrates in S-III and S-II samples .While S-I contains iron whose oxides remains stable at high temperatures.

4.1 DESCRIPTION OF EQUIPMENT

The equipment used was SEM-JSM-6510LV JEOL. This SEM is widely used in industrial applications. In this technique a high beam of electrons is made to strike on the sample to be analysed. These electrons interact with the sample being studied and produce different images.



Fig 4.1 SEM-JSM-6510LV JEOL MODEL

4.2 EXPERIMENTAL PROCEDURE

Leaching was carried out on three Fly and Bottom ash samples through TCLP. TCLP consists of four fundamental procedures:

- Sample preparation for leaching
- Sample leaching
- Preparation of leachate for analysis

➤ Leachate analysis.

For liquid wastes containing less than 0.5 percent %age of dry solid component the extract after filtration through a 0.5 to 0.9 micron (μm) glass fiber filter, is defined as the TCLP extract

In the TCLP procedure the pH of the sample material is first established, and then leached with an acetic acid solution at a 1:20 mix of sample to solvent. For example, a TCLP jug may contain 1g of sample and 20 mL of solution. The resulting leachate mixture is then sealed in extraction vessel for general analyses, or possibly pressure sealed for volatile organic compounds and thrown together for 18 hours to simulate an extended leaching time in the ground. It is then filtered so that only the solution remains and this is then analyzed.

4.3 ATOMIC ABSORPTION SPECTROSCOPY (AAS)

This method is used for obtaining the concentration of a particular element in a sample to be analyzed. AAS can be used to determine many different elements in solution or in solid samples used in various types of research. In this method light energy of particular wavelength is captured by ground state atom after it enters in the excited state. The captured amount of light is increased with the increase in number of atoms present in the light path. The right selection of wave length and good source of light allow for determination of the individual element.



Fig. 4.2 Atomic absorption spectrophotometer (Make: GBC)

4.4 SEM ANALYSIS OF FLY ASH LEACHATES

Following SEM micrograph images tells about the effect of leaching on fly and Bottom Ash samples. Magnification was done at 2000X.

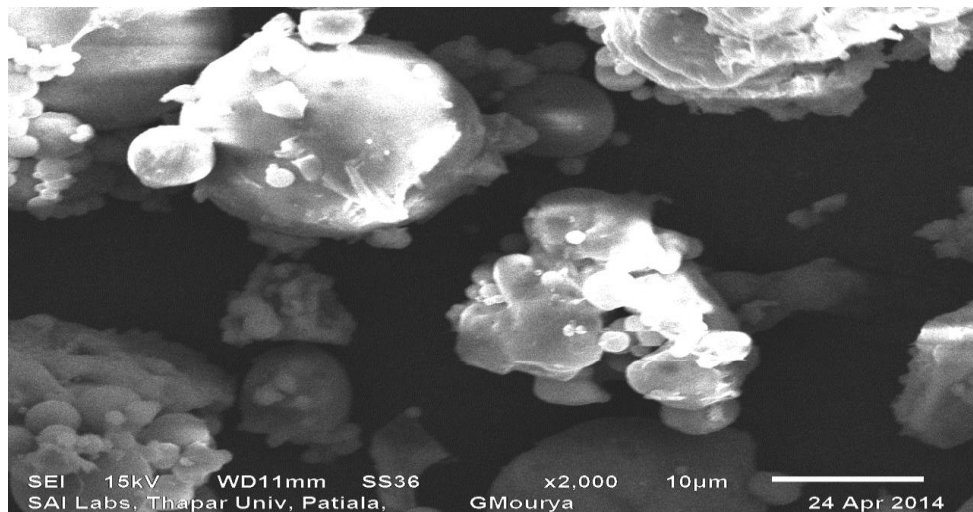


Fig. 4.3 SEM analysis of S-III leachate(2000X)

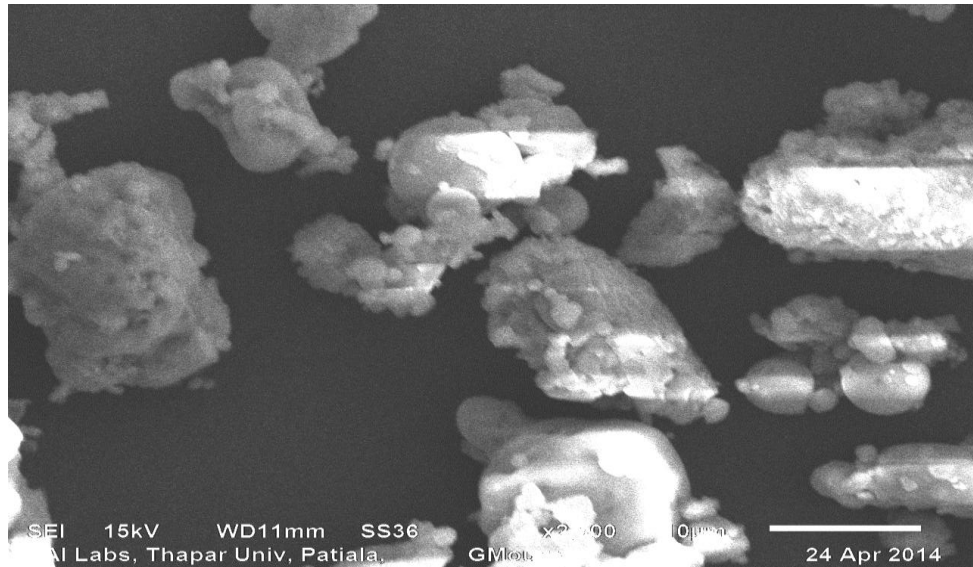


Fig. 4.4 SEM analysis of S-I leachate(2000X)

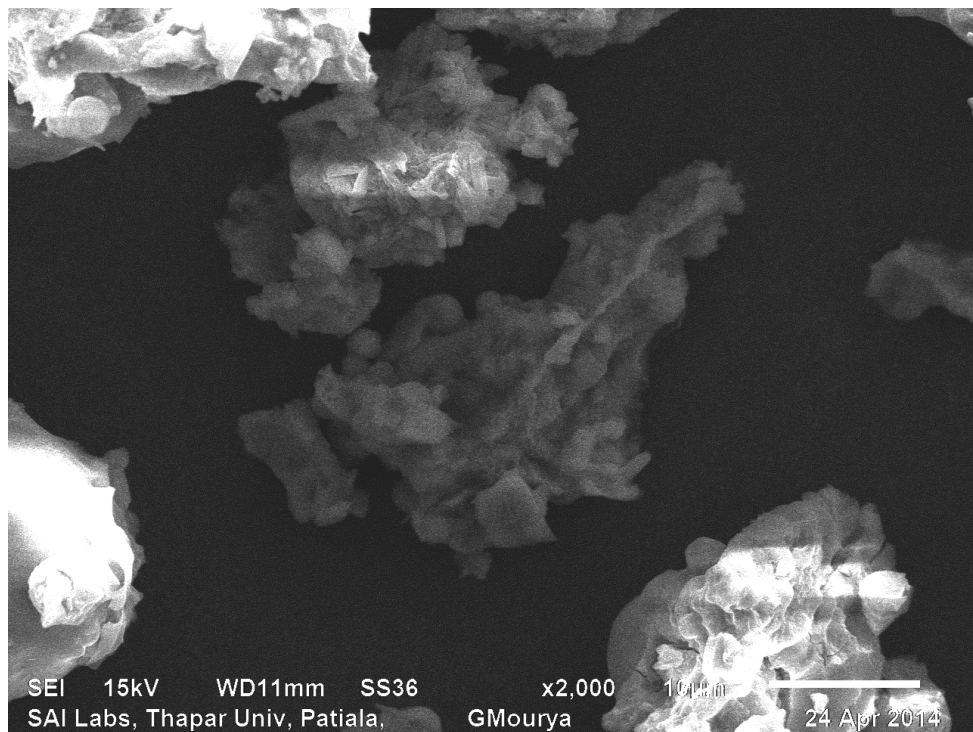


Fig. 4.5 SEM analysis of S-II Fly ash leachate (2000X)

From the SEM analysis carried out on three fly ash samples ,it showed the changes in morphology from uniform ,spherical particles(in case of non –leachates) to less uniform, irregular and coarse particles with changes in shape and size. Also changes in color were noticed in all three samples which signify the removal of elements due to leaching. Spherical fly ash particles are visible with little crystal structure formation or variation in their general shapes (lumps) occur as compared to non-leachates which signifies the effects due to leaching. Evidence of high unburnt carbon are also visible.

4.5 EDS ANALYSIS OF FLY ASH LEACHATE SAMPLES

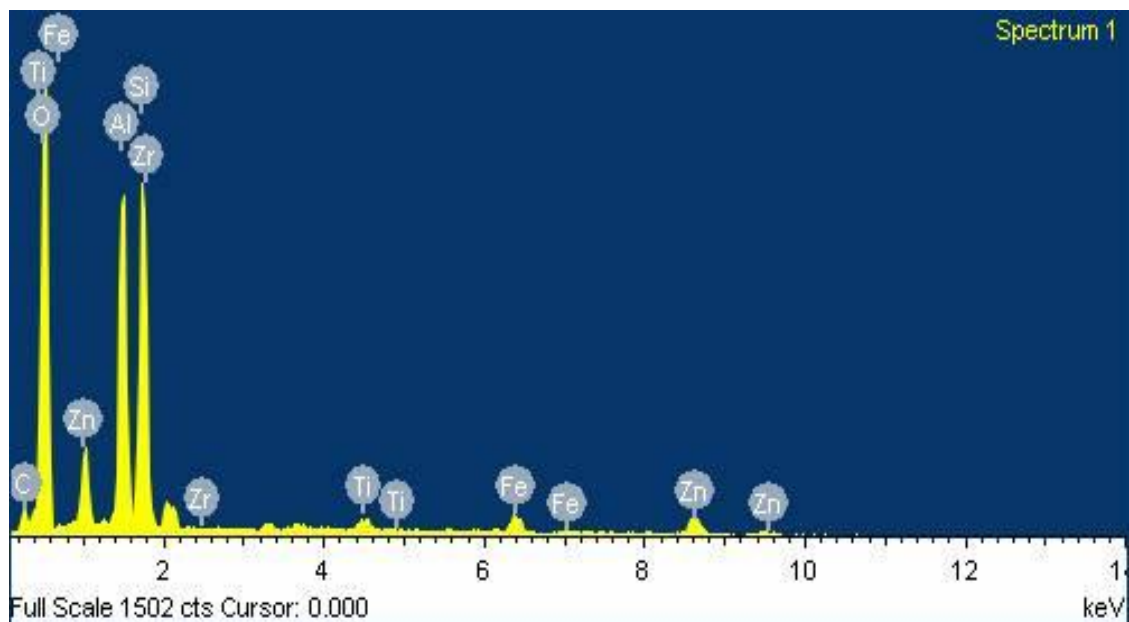


Fig. 4.6 EDS spectrum of S-III Fly Ash leachate

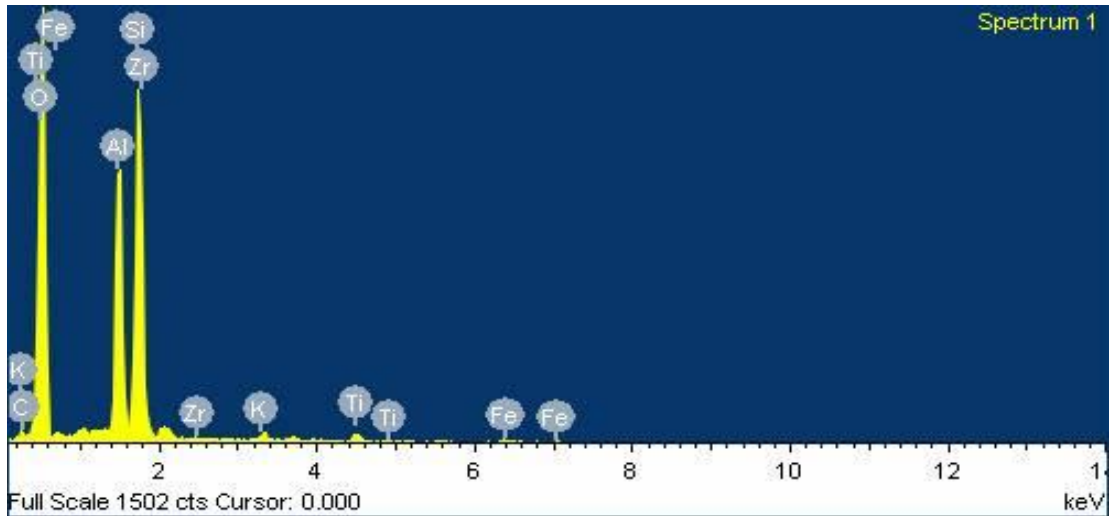


Fig. 4.7 EDS spectrum of S-I Fly Ash leachate

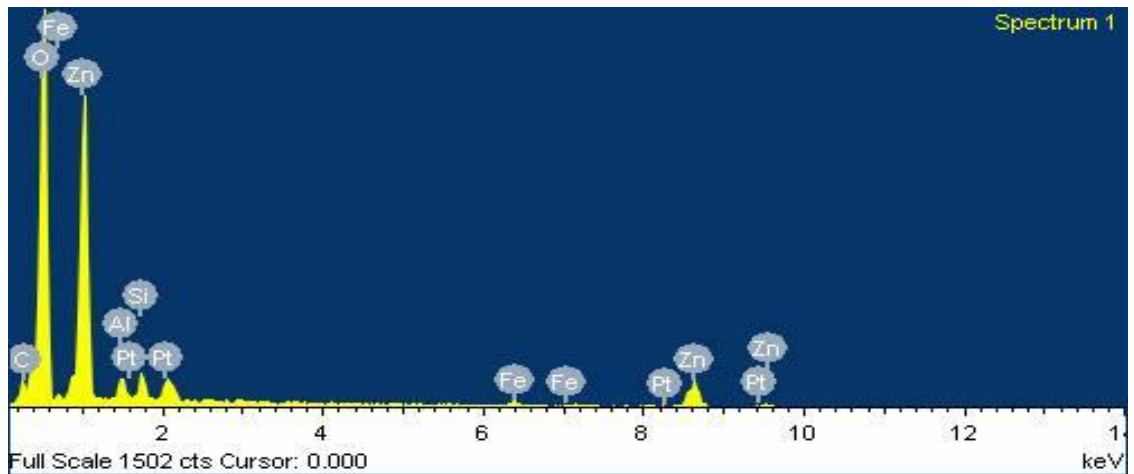


Fig. 4.8 EDS spectrum of S-II Fly Ash leachate

The corresponding EDS data suggest that aluminum, oxygen, titanium, zinc, zirconium iron, and silicon are the primary elements at the point of analysis. From the EDS data of S-III fly ash leachate it showed significant amount of carbon (6.91%). This may be due to the increase in carbon content which may arise due to the formation of amorphous or crystalline carbonate minerals in the fly ash leachate. This indicates carbonation of fly ash particles.

The Graph shows that 11.30 % of aluminum is present in S-III Fly ash leachate as compared to 15.74% of aluminum in S-III fly ash without leaching .Thus Leaching rate of aluminum is 28.2% which signifies that 28.2% of aluminum was leached from the S-III Fly ash under TCLP test.Similarly 31.5% of silicon was leached from total fly ash under TCLP test.Element Zirconium too showed reduction in content due to leaching.From the EDS data of S-III fly ash leachate it showed significant amount of carbon (8.21%) in comparison to it non –leachate. This is due to the reason explained above. Also reduction in metal content is noticed in some metals(C, Al, Si, and Fe).Following Table 4.1 shows Chemical Composition of all three samples of Fly ash leachates.

Table 4.1 Chemical Composition of Fly Ash Leachates

Element	S-III fly ash leachate(%weight)	S-I fly ash leachate(%weight)	S-II fly ash leachate (%weight)
C	6.91	8.24	7.18
O	56.56	63.45	69.20
Al	11.30	10.43	1.60
Si	13.22	14.91	1.76
Ti	0.73	0.69	-
Fe	2.40	0.55	0.95
Zn	5.92	-	14.58
Zr	2.95	1.41	-
K	-	0.33	-
Pt.	-	-	4.73

Above Table shows that Oxygen, Silicon and Aluminum dominates the list of elements in the Leachates. It was observed that S-II fly ash leachate contained traces of aluminum and Silicon in contrast to S-III and S-I Fly ash leachates where they are mostly present. Ropar fly ash leachate in comparison to its non-Leachate form (S-II fly ash) leaches out most

number of elements. S-III Fly ash leaching rate for Silicon is 31.5% while for S-I and S-II is 27.9% and 92% respectively while leaching rate for aluminum content of S-III, S-I and S-II Fly ash are 28.2%, 13.1% and 88.6%. S-II fly ash leachate shows maximum leach ability (94.2%) while S-III and S-I leaches out 30.8% and 8.1% of Silicon respectively.

4.6 EDS ANALYSIS OF BOTTOM ASH LEACHATE SAMPLES

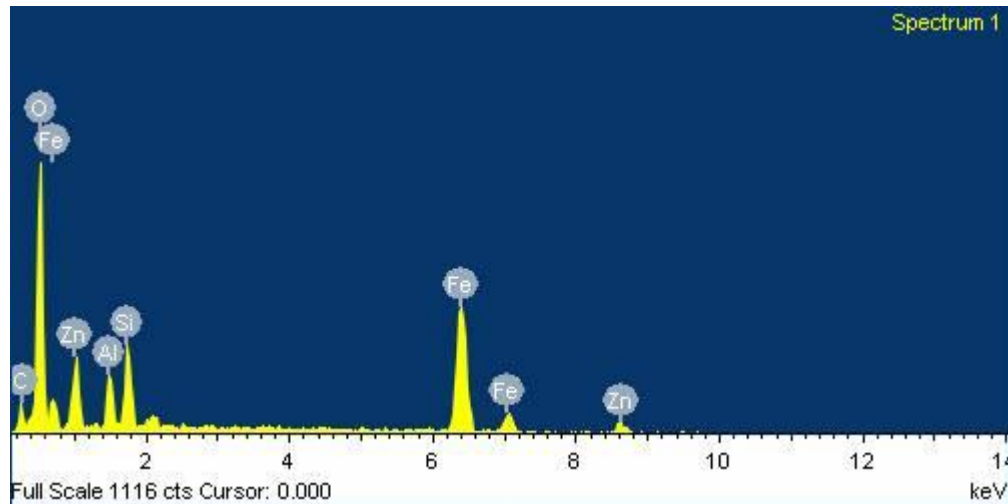


Fig. 4.9 EDS spectrum of S-III Bottom Ash Leachate

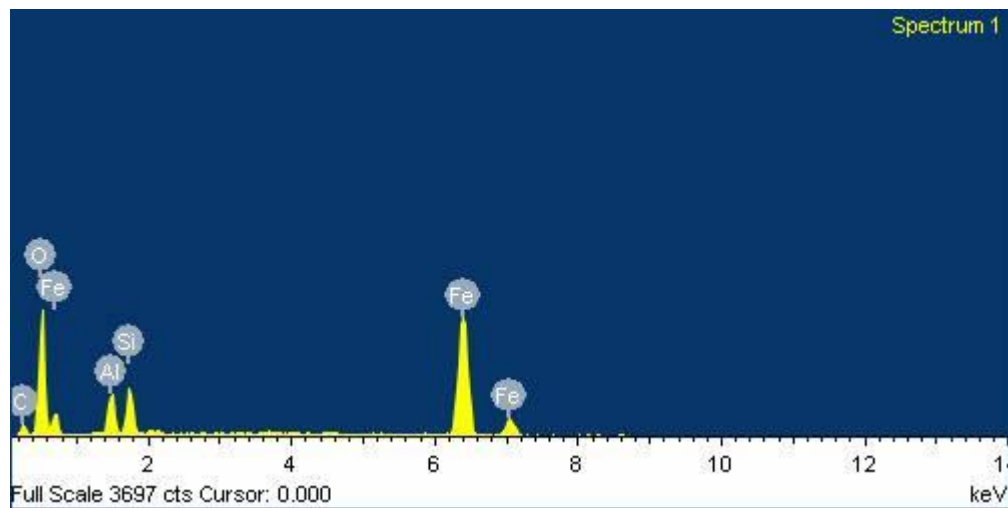


Fig. 4.10 EDS spectrum of S-I Bottom Ash Leach

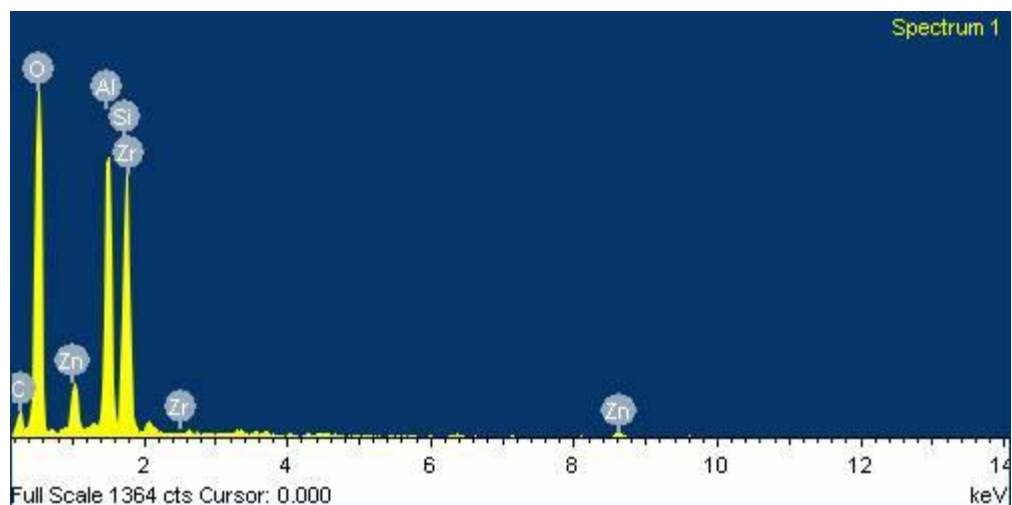


Fig. 4.11 EDS spectrum of S-II Bottom Ash Leachate

Table 4.2 Chemical Composition of Bottom Ash Leachates

Element	S-III bottom ash leachate(%weight)	S-I bottom ash leachate(% weight)	S-II bottom ash leachate(%weight)
Carbon	13.31	10.04	11.70
Oxygen	44.64	34.48	59.03
Aluminum	3.45	4.97	12.51
Silicon	5.06	5.00	12.91
Iron	27.98	45.51	-
Zinc	5.56	-	2.14
Zirconium	-	-	1.71

The corresponding EDS data suggest that Carbon, oxygen, Aluminum, Silicon are the primary elements at the point of analysis of leachates of Bottom ash. S-III Bottom ash leachate showed large amounts of unburnt carbon (13.31%) whereas S-II contained least unburnt carbon (11.70%). Also S-III bottom ash leachate leaching rate for aluminum is 77.78% and that of Silicon is 75%.

4.7 SEM IMAGES OF BOTTOM ASH LEACHATES

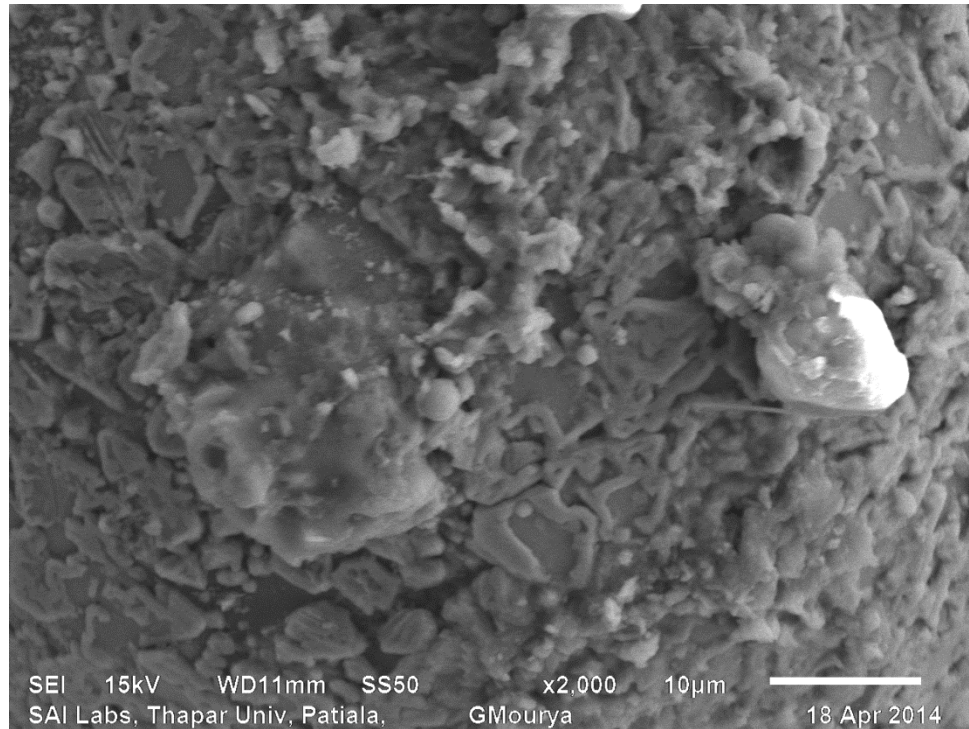


Fig.4.12 SEM image of S-III bottom ash leachate



Fig.4.13 SEM image of S-I bottom ash leachate

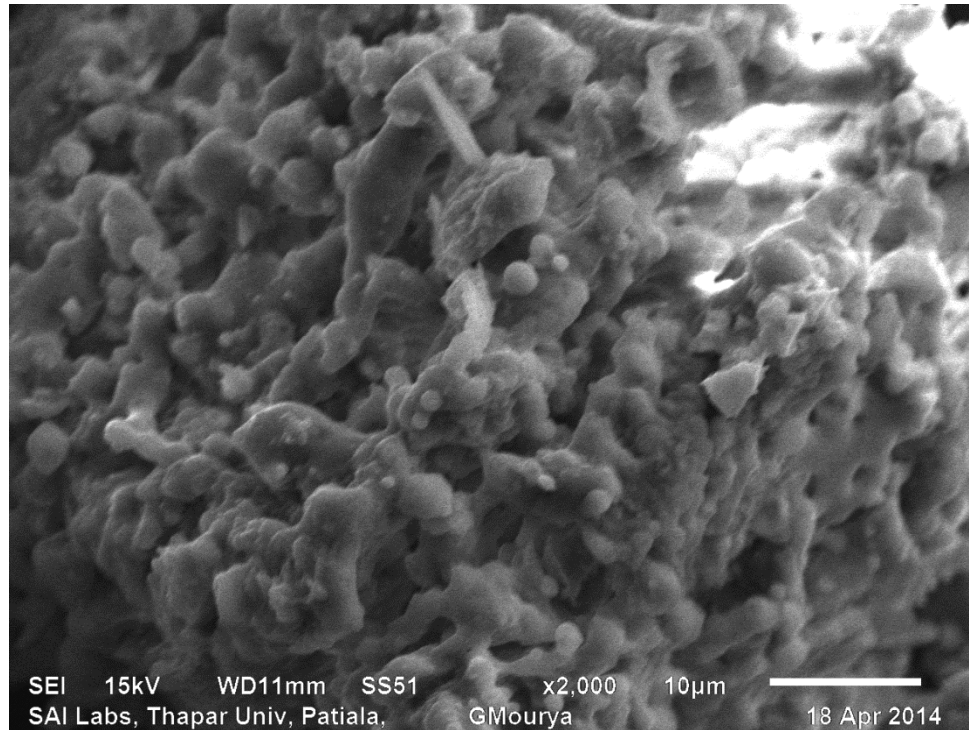


Fig.4.14 SEM image of S-II bottom ash leachate

From the SEM analysis carried out on three Bottom ash samples, it showed the changes in morphology from uniform, spherical particles (in case of non-leachates) to less uniform, irregular and coarse particles with changes in shape and size. In case of S-I Bottom ash leachate, there is change in its morphology as its leachate now consists of clusters of particles clubbed together. Spherical fly ash particles are visible with little crystal structure formation or variation in their general shapes (lumps) occur as compared to non-leachates which signifies the effects due to leaching. Nevertheless change in structure is clearly visible in all three samples.

Fig. 4.15 AAS results of S-III fly ash leachate

S.No	Elements	Unit	Results
1.	Pb	mg/l	0.75
2.	Zn	mg/l	1.96
3.	Cu	mg/l	0.34
4.	Fe	mg/l	34.84
5.	Ni	mg/l	0.57
6.	Mn	mg/l	0.58
7.	Al	mg/l	168.9
8.	Cr	mg/l	0.19
9.	Cd	mg/l	0.04

These results obtained were compared to standard reference. In this test we have taken drinking water as a standard reference. Now as Coal ash gets leached inside groundwater, there is chance that underground water reserves may get polluted. Thus need arises for comparing these test results with the IS:10500 limit on drinking water.

Table 4.3 IS: 10500 limit on drinking water

Element	IS:10500 Limit(mg/l)
Pb	0.05
Al	0.2
Cd	0.01
Cr	0.05
Ni	0.02
Zn	15
Mn	0.5
Cu	1.5

Thus from above Fig. we see that concentrations of Pb, Cd and Ni in the above S-III fly ash leachate exceeds IS: 10500 limit on drinking water whereas rest of other elements were under maximum permissible limit.

During the study it was observed after performing the experimental analysis of S-III fly ash leachate that the elements leached such as Pb and Cd have profound effects on human health and environment. These elements have the tendency to pollute underground water sources, thereby making them unfit for human consumption. Other elements such as Zn, Al, Fe, and Ni were also leached but in minute quantities as per the AAS result, but these elements concentration were found to be within maximum acceptable criteria in accordance with the IS:10500 standards for quality drinking water. Also after performing experimental analysis of coal ash leachates, changes were observed in morphology of coal ash. This was caused due to effects of leaching. It was also found that Aluminum and Silicon were the most leached elements from both the samples of coal ash.

5.1 FUTURE SCOPE

The main aim of the present study was to investigate the Leaching behavior of Coal ash using SEM (Scanning Electron Microscopy), EDS (Energy dispersion spectroscopy) and to study coal ash physical properties such as particle size distribution, XRD (X-ray diffraction), DTA (Diffraction Thermal Analysis). The various works that can augment the present study are:

- Using leaching properties of Coal ash to calculate extraction efficiency of various metals.
- Extraction of Quartz from the coal ash.
- Use of fly ash for substituting Cement in Construction industry. .

There is still a large scope for further research in this field of Coal Ash technology for its efficient utilization. Coal ash has many uses and has the potential for being used as replacement to many materials. It can help to minimize the problem of resource depletion. There are several other applications that would use good quantity of fly ash and would yield economic returns / savings. These include use of fly ash in roller compacted

concrete, hydraulic structures, reclamation of low lying areas, fly ash based wood substitute, fly ash based granite substitute, tiles, aggregates, zeolites, paints and enamels etc.

REFERENCES

1. Sakorafas, C.; Michailidis, K.; Burrigato, F. (1995) "Physical, Chemical, Mineralogical and Thermal properties of Cenospheres from ash lagoon. Chemistry of Megalopolis Lignite Fly ash", *Fuel*, 75, 419-423.
2. Stanislav, V.; Vassileva, G. (1995) "Mineralogy of combustion wastes from coal-fired powerstations", *Fuel Processing Technology*, 47, 261-280.
3. Bayat, O. (1997) "Characterization of Turkey Fly Ash". *Fuel*, 77, 1059-1066.
4. Swapan, K.; Mallick, D.; Dutta, N.S.; Chaudhri, K.S. (1997) "Studies on the phase mineralogy leaching characteristics of coal fly ash." *Fuel*, 107, 251-275.
5. Nathan, Y.; Dvorachek, M.; Pelley, I.; Mimran, U. (1998) "Characterization of coal fly ash from Israel", *Fuel*, 78, 205-213.
6. Henry, A.F.; Thomas, L.R.; James, C. H.; Graham, U.M. (1998) "Characterization of fly ash from Israel", *Fuel Technology*, 78, 215-233.
7. Kolay, P.K.; Singh, D.N. (2000) "Physical, chemical, mineralogical, and thermal properties of cenospheres from an ash lagoon", *Cement and Concrete research*, 31, 531-542.
8. Choi, S.K.; Lee, S.; Song, Y.K.; Moon, H.S. (2002) "Leaching characteristics of Korean Fly Ash and its implications on groundwater composition", *Fuel Technology*, 81, 1083-1091.
9. Moreno, N.; Querol, X.; Andres, J.M.; Stanton, K.; Towler, M.; Nugteren, H.; Janssen-Jurkovicova, M.; Jones, R. (2004) "Physio-chemical characteristics of European pulverized

coal combustion fly ashes”, *Fuel Technology* ,84, 1351-1363.

10. Grochowiak,K.S.Gólas; Jankowski ,J.H.;Kozin ,S. (2004) “Characterization of the coal fly ash: improvement of industrial on-line measurement of unburned carbon content”,*Fuel*, 83, 1847-1853.

11. Goodarzi,F. (2005) “Morphology and chemistry of fine particles emitted from a Canadian power plant”,*Fuel*, 85, 273-280.

12. Brodowski,S.; Amelung,W.; Haumaier,L.;Clarissa ,A.; Zec,W. (2005) “Morphological and chemical properties of black carbon using SEM and EDX”, *geoderma*, 128, 116-129.

13. Ural,S. (2005) “Comparison of fly ash properties from Afsin–Elbistan coal basin”. *Journal of hazardous materials* ,119, 85 -92.

14. Sarkar,A;Rano,R.; Udaybhanu ,G.;Basu, A.K.(2005) “A comprehensive characterisation of fly ash from a thermal power plant in Eastern India”, *Fuel Processing Technology*,87, 259-277.

15. Blanco, F.; Garcia, M.P.; Ayala, J.; Mayoral,G.; Garcia,M.A.(2006) “The effect of mechanically and chemically activated fly ashes on mortar properties”,*Fuel*, 85, 2018–2026.

16.Goodarzi,F. (2006) “Characteristics and composition of fly ash from Canadian coal-fired power plants”, *Fuel* ,85, 1418-1428.

17.Kutchko,B.G.;Kim,A.G.(2006) “Fly ash characterization by SEM–EDS”, *Fuel*,85, 2537–2544.

18. Koukouzas ,N. K.;Zeng .R.;Perdikatsis.V.;Xu .W.;Kakaras .E.K. (2006) “Mineralogy and geochemistry of Greek and Chinese coal fly ash,” *Fuel*, 85, 2301–2309.

19. Nikolaos ,K.; Papanikolaou,D.; Tourunen,A.; Janitti,T.(2007) “Mineralogical and elemental composition of fly ash from pilot scale fluidized bed combustion of lignite, bituminous coal, wood chips and their blends”, *Fuel*, 86, 2186-2193.
20. Liu,Y.; Gupta,R.; Elliot,L.; Wall,T.; Fujimori,T.(2007) “Thermo mechanical analysis of laboratory ash, combustion ash and deposits from coal combustion”,*Fuel Processing Technology*, 88, 1099-1107.
21. Izquierdo ,B.M.T.; Mayoral, M.C.; Bona M.T.;Martínez-Tarazona, R.M. (2007) “Preparation and characterization of carbon-enriched coal fly ash”, *Journal of environmental management*, 88, 1562-1570.
22. Xiaoru ,F.; Li,Q.;Zhai,J, Sheng,G.; Li,F. (2007) “The physical–chemical characterization of mechanically-treated CFBC fly ash”, *Cement and Concrete Composites*, 30, 220-226.
23. Dutta ,B. K.;Khanra ,S., Mallick.D. (2009) “Leaching of elements from coal fly ash: Assessment of its potential for use in filling abandoned coal mines”, *Fuel*, 88, 1314-1323.
24. Ahmaruzzaman ,M. (2009) “Review on the utilization of fly ash”, *Progress in energy and combustion sciences*, 36, 327–363.
- 25.Mishra,D.P.;Das ,S .K. (2010) “Study of physio-chemical and mineralogical properties of Talcher coal fly ash for stowing in underground coal mines”, *Material Characterization*, 61, 1252-1259.
- 26.Zahi S.; Daud, A.R. (2010) “Fly ash characterization and application in Al–based Mg alloys ”, *Materials and design* , 32, 1337–1346 .

27. Sarode, D.B.; Jadhav, R.N.; Khatik, A.V.; Ingle, T.S.; Attarde, S.B. (2010) “Extraction of heavy metals from Thermal Power Plant Fly ash”, *Polish J. Inst. of environ. Stud*, 19, 1325-1330.
28. Bhattacharjee, A.; Mandal, H.; Roy, M.; Kusz, J. (2011) “Microstructural and magnetic characterization of fly ash from Kolaghat Thermal Power Plant in West Bengal, India. *Journal of magnetism and magnetic materials*”, 323, 3007-3012.
29. Chengu, W.U.; Hongfa, Y.U.; Huifang, Z. (2012) “Extraction of aluminum by pressure acid-leaching method from coal fly ash”, *Trans. non-ferrous Met. Soc. China*, 22, 2282-2288.
30. Singh, R.K.; Gupta, N.C.; Guha, B.K. (2012) “Leaching Characteristics of trace elements in fly ash and ash disposal system. *Energy Sources*”, 34, 602-608.